Redox Biology 28 (2020) 101389

Contents lists available at ScienceDirect

Redox Biology

journal homepage: www.elsevier.com/locate/redox

Research Paper

Monosodium luminol reinstates redox homeostasis, improves cognition, mood and neurogenesis, and alleviates neuro- and systemic inflammation in a model of Gulf War Illness

Ashok K. Shetty*,[1], Sahithi Attaluri[1], Maheedhar Kodali[1], Bing Shuai[1], Geetha A. Shetty, Dinesh Upadhya[2], Bharathi Hattiangady, Leelavathi N. Madhu, Raghavendra Upadhya, Adrian Bates, Xiaolan Rao

Institute for Regenerative Medicine, Department of Molecular and Cellular Medicine, Texas A&M University College of Medicine, College Station, TX, USA

ARTICLE INFO

Keywords:
Anhedonia
Anxiety-like behavior
Gulf War Illness
Hippocampal neurogenesis
Memory
Monosodium luminol
Mood dysfunction
Neuroinflammation
Oxidative stress
Reactive Oxygen Species

ABSTRACT

Enduring brain dysfunction is amid the highly manifested symptoms in veterans with Gulf War Illness (GWI). Animal studies have established that lasting brain dysfunction in GWI is concomitant with augmented oxidative stress, inflammation, and declined neurogenesis in the brain, and systemic inflammation. We hypothesize that drugs capable of restoring redox homeostasis in GWI will improve cognitive and mood function with modulation of neuroinflammation and neurogenesis. We examined the efficacy of monosodium luminol-GVT (MSL), a drug that promotes redox homeostasis, for improving cognitive and mood function in GWI rats. Young rats were exposed to GWI-related chemicals and moderate restraint stress for four weeks. Four months later, GWI rats received different doses of MSL or vehicle for eight weeks. Behavioral analyses in the last three weeks of treatment revealed that GWI rats receiving higher doses of MSL displayed better cognitive and mood function associated with reinstatement of redox homeostasis. Such restoration was evident from the normalized expression of multiple genes encoding proteins involved in combating oxidative stress in the brain and the return of several oxidative stress markers to control levels in the brain and the circulating blood. Sustained redox homeostasis by MSL also resulted in antiinflammatory and pro-neurogenic effects, which were apparent from reduced densities of hypertrophied astrocytes and activated microglia, and increased neurogenesis with augmented neural stem cell proliferation. Moreover, MSL treatment normalized the concentration of multiple proinflammatory markers in the circulating blood. Thus, MSL treatment reinstated redox homeostasis in an animal model of GWI, which resulted in alleviation of both brain and systemic inflammation, improved neurogenesis, and better cognitive and mood function.

1. Introduction

Gulf War Illness (GWI) afflicts over a third of 700,000 veterans who served in the first Gulf War [1]. The brain-related symptoms in GWI comprise difficulties in learning, making new memories, and depressive- and anxiety-like behavior [2–4]. These symptoms are linked with continuing alterations in the structure and function of the brain [5–8]. Exposures to various chemicals during the war have been suggested as the likely cause of GWI. These include pyridostigmine bromide (PB, reversible acetylcholinesterase [AChE] inhibitor), and a variety of pesticides [9]. The pesticides include the insecticide permethrin (PER) and the insect repellant DEET [1,10]. The occurrence of GWI is also higher in veterans who employed pesticides and/or consumed PB pills at higher levels [10–12]. The other possible causes of GWI comprise exposure to sarin, depleted uranium, and smoke from the fire in oil wells.

Thus, the symptoms exhibited by a vast majority of GW veterans are likely due to synergistic interaction of PB with pesticides (PER and

* Corresponding author. Institute for Regenerative Medicine, Texas A&M Health Science Center, College of Medicine, 1114 TAMU, 206 Olsen Boulevard, College Station, TX, 77843, USA.
E-mail address: akskrs@tamu.edu (A.K. Shetty).
[1] AKS, SA, MK and BS contributed equally to this work.
[2] *Current address of Dinesh Upadhya:* Centre for Molecular Neurosciences, Kasturba Medical College, Manipal Academy of Higher Education, Manipal, Karnataka, India.

https://doi.org/10.1016/j.redox.2019.101389
Received 20 September 2019; Received in revised form 12 November 2019; Accepted 15 November 2019
Available online 18 November 2019

DEET) or interaction of a cocktail of multiple chemicals with stress [1,10,13]. Studies in a rat model have suggested that exposure to low-moderate doses of chemicals PB, PER and DEET, and mild-moderate stress for 4 weeks can induce blood-brain barrier disruption, astrocyte hypertrophy, activated microglia, and decreased AChE activity [14–18]. Studies evaluating the effects of exposure to higher doses of PB and PER in mouse models have also reported astrocyte hypertrophy, changes in proteins related to lipid metabolism, molecular transport, the endocrine and immune systems, memory impairment, and anxiety or disinhibition-like behavior [19,20]. Comparable observations have also been made in other animal prototypes of GWI, which used exposures to various combinations of different GWI related chemicals [21–23].

Gulf War veterans display brain dysfunction and an increased incidence of memory and mood impairments [3,5,24–27]. Likewise, studies in a rat model of GWI have shown that combined exposure to PB, PER, and DEET for four weeks with mild or moderate stress causes persistent cognitive and mood impairments [16–18,28]. Interestingly, such brain impairments were associated with incessantly increased oxidative stress, neuroinflammation, and declined neurogenesis, as well as systemic inflammation [17,18,29]. Because the brain function is sensitive to elevated levels of reactive oxygen species (ROS) and proinflammatory conditions [30,31], sustained oxidative stress, neuroinflammation, and systemic inflammation are likely among the leading causes of unremitting cognitive and mood impairments in GWI. It remains to be uncovered in GWI whether oxidative stress precedes chronic inflammation or vice versa, however. It is plausible that the augmented oxidative stress is the underlying cause of chronic inflammation in GWI because most GWI-related chemicals are acetylcholinesterase inhibitors, which are known to induce oxidative stress in cells [32]. Excessive ROS and the associated protein oxidation and damage of cellular components can initiate the release of inflammatory signaling molecules and interfere with the synaptic communication between neurons. Oxidative stress also promotes the cellular release of the high mobility group protein B1 (HMGB1) from neurons, glial and endothelial cells, leading to HMGB1 and toll-like receptor 4 (TLR4) axis activation [33,34]. Indeed, HMGB1 leakage into the extracellular space has been observed in a model of GWI [18].

We hypothesize that drugs capable of restoring redox homeostasis in GWI will improve cognitive and mood function with modulation of neuroinflammation and neurogenesis. Therefore, we rigorously investigated the beneficial effects of treating GWI rats with monosodium luminol-GVT (MSL, Bach Pharma, Inc., North Andover, MA), a drug that has previously shown promise for improving redox homeostasis in several animal prototypes of disease [35–40]. Our results demonstrated that the administration of higher doses of MSL to GWI rats reinstated redox homeostasis in the brain as well as the circulating blood, which resulted in better cognitive and mood function associated with the alleviation of both brain and systemic inflammation, and improved neurogenesis.

2. Materials and methods

2.1. Animals

Approximately 2.5-month old male Sprague Dawley rats (n = 75; Harlan, Indianapolis, IN) were housed with continuous access to food and water for 10 days. The rats were then randomly assigned to either the naïve control group (n = 15) or the GWI group (n = 60). The animal care and use committee of the Texas A&M Health Science Center College of Medicine approved all studies conducted in this investigation.

2.2. Exposure of animals to GWIR-chemicals and restraint stress

The animals assigned to the GWI group (n = 60) received PB (2 mg/kg, oral; Sigma, St. Louis, MO), DEET (200 μl, 60 mg/kg, dermal; Chem Service Inc, West Chester, PA), and PER (200 μl, 0.2 mg/kg, dermal; Chem Service Inc), and 15 min of restraint stress daily for 28 days, as described in our previous studies [16,17,29]. Age-matched naïve control animals (n = 15) were maintained in parallel with GWI animals but not subjected to chemical and stress exposure. The choice of chemicals and the exposure regimen employed in this study are based on epidemiological studies implying that GWI in a significant percentage of GW veterans is an outcome of consumption of PB and exposure to insect repellants and insecticides such as DEET and PER, and interaction of these chemicals with war-related stress (1, 10). In this study, we employed relatively lower doses of PB, DEET, and PER using routes that simulated the exposure experienced by most veterans during the GW (i.e., PB orally; and PER and DEET dermally). A report by the research advisory committee (RAC) on GWI implied that the overall incidence of GWI is higher in veterans who used higher amounts of these chemicals than veterans who had limited exposure during the GW (10). In some veterans, a higher level of exposure to such chemicals was also associated with higher consumption of PB pills (10–11). Based on the estimate by the Department of Defense, a significant number of military personnel took two 30 mg tablets of PB per day during the GW [41]. However, the exact amount of PER or DEET used during the GW is unknown as soldiers liberally used these chemicals on the skin, and their uniforms (10). While it is difficult to directly compare the doses of chemicals and the amount of stress employed in an animal model in this study to those experienced by the veterans during the GW, the employed dosages did produce the phenotype of GWI, particularly the occurrence of persistent cognitive and mood impairments, and chronic inflammation at extended time-points after the exposure (18). Also, no mortality was seen during or immediately after the exposure to these chemicals.

2.3. Treatment of GWI animals with MSL

Four months after exposure to GWIR-chemicals and stress, GWI-rats were randomly assigned to four groups: a group receiving vehicle (GWI-VEH group, n = 14), and three groups receiving MSL at 40, 80 and 160 mg/kg (GWI-MSL 40 mg/kg; GWI-MSL 80 mg/kg; GWI-MSL 160 mg/kg groups, n = 13–14/group). Animals in the GWI-VEH group received sterile water (500 μl, oral) whereas, animals in GWI-MSL groups received MSL dissolved in 500 μl sterile water orally at the respective doses mentioned above for 8 weeks (5 days/week). The dose of MSL employed in this study was based on a previous study where 150 mg/kg/day oral dose of MSL for over two months considerably reduced oxidative stress and corrected neuromotor deficits in a model of Ataxia telangiectasia [38]. To examine dose-response effects, we tested the effects of 3 doses, 40, 80, or160 mg/kg (oral) in this study. The animals also received injections of 5′-bromodeoxyuridine (BrdU, daily for 5 days) in the third week of vehicle or MSL treatment, and subjected to a series of behavioral tests in the last three weeks of the treatment period. We gave BrdU in the 3rd week of treatment to examine whether short-term (3-weeks) treatment of MSL is sufficient for improving neurogenesis in this model. Age-matched naïve control animals did not receive MSL/vehicle treatment but subjected to similar BrdU injections and behavioral testing at time-points matching the GWI groups.

2.4. Analysis of hippocampus-dependent cognitive function

An object location test (OLT), a hippocampus-dependent cognitive test, was utilized to characterize the ability of animals to discern minor changes in the environment, as detailed in our previous studies [17,28]. Briefly, the test comprised three trials (T1, habituation trial; T2, sample trial; T3, test trial), each of which lasted 5 min and the inter-trial interval (ITI) was 30 min (Fig. 1 [A1]). The animals explored two identical objects placed on opposite sides of the box in T2, whereas, in T3,

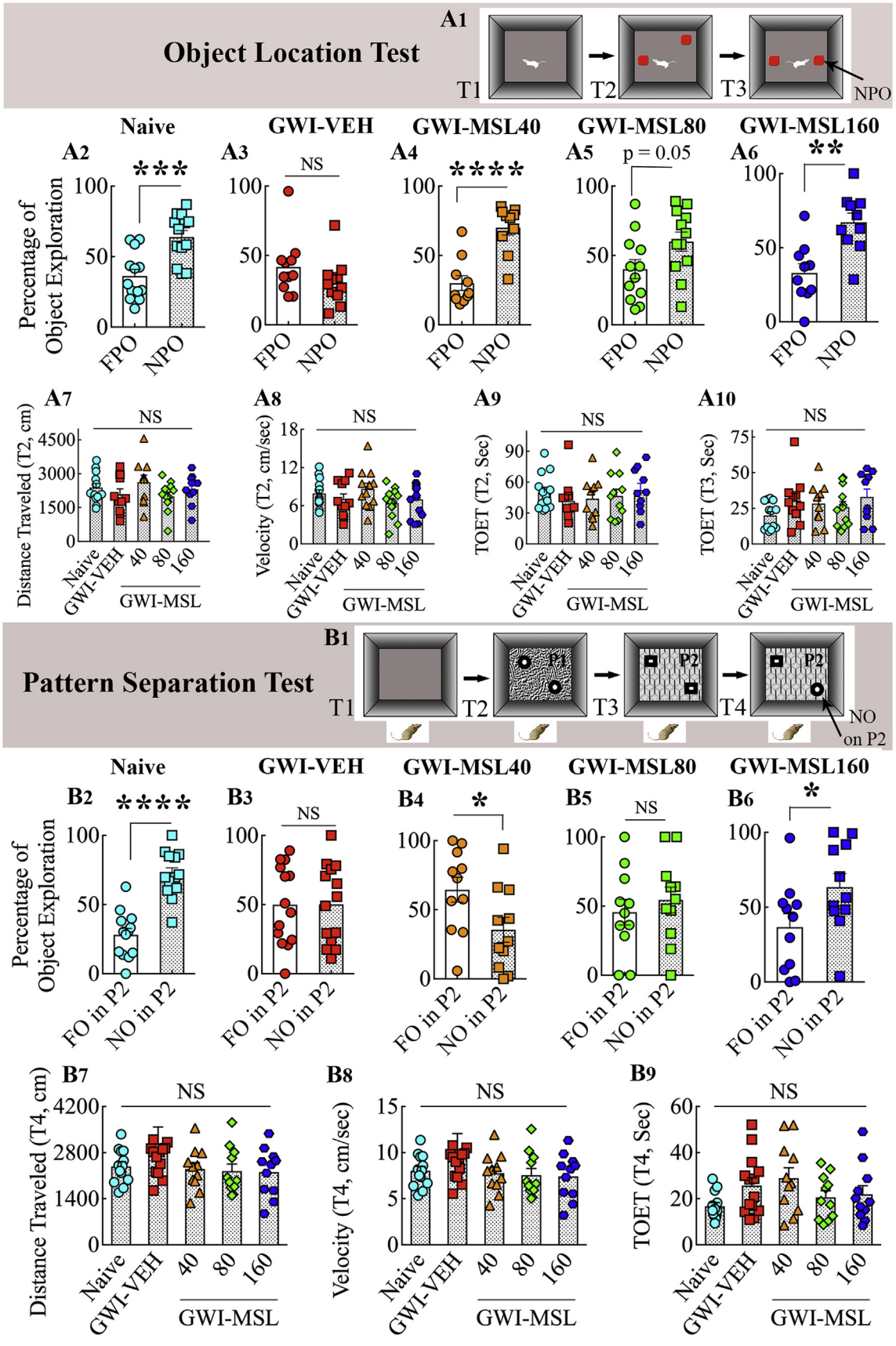

(caption on next page)

Fig. 1. Monosodium Luminol (MSL) treatment to rats with Gulf War Illness (i.e., GWI rats) improved their ability for discerning minor changes in the environment and pattern separation. The upper half of the figure displays the results of an object location test (OLT). A1 shows the various phases involved in this test whereas, the bar charts in A2-A6 show the performance of animals belonging to naïve control (Naive, A2), GWI animals receiving vehicle (GWI-VEH, A3), and GWI animals receiving different doses of MSL (GWI-MSL40, GWI-MSL80, GWI-MSL160; A4-A6). Animals in the GWI-VEH group were impaired (A3), which was evident from their lack of preference for the novel place object (NPO) over the familiar place object (FPO). In contrast, animals in naïve control and GWI-MSL groups showed better cognitive function, which was apparent from their preference for NPO in OLT (A4-A6). The bar charts in A7-A10 compare parameters such as the distance traveled (A7), the velocity of movement (A8), or the total object exploration times (TOETs, A9-A10). $^{**}p < 0.01$, $^{***}p < 0.001$, $^{****}p < 0.0001$; NS, not significant; T1-T3, trials 1–3. The lower half of the figure illustrates the results of a pattern separation test (PST). B1 shows the various trials involved in this test whereas, the bar charts in B2–B6 show the performance of animals belonging to naïve (B2), GWI-VEH (B3), and GWI-MSL (B4–B6) groups. Animals belonging to GWI-VEH, GWI-MSL40, and GWI-MSL80 groups were impaired (B3, B4, B5), which was evident from their lack of preference for the novel object on pattern 2 (NO on P2) over the familiar object on pattern 2 (FO on P2). In contrast, animals belonging to naïve control (B2) and GWI-MSL160 (B6) groups displayed pattern separation ability, which was apparent from their preference for exploring for NO on P2 or FO on P2. The bar charts in B7–B9 compare parameters such as the distance traveled (B7), the velocity of movement (B8), or the TOET (B9). *, $p < 0.05$, and ****, $p < 0.0001$; NS, not significant; T1-T3 trials 1–3.

the animals explored the same objects with one of the objects remaining in its location, and the other object moved to a new location in the open field. The movement of the rat in T2 and T3 were video-tracked using Anymaze software. The soundness of this test hinges on the attentive exploration of the two objects and their locations in T2 (Fig. 1 [A1]). Therefore, we set an inclusion criterion that required at least 16 s of object exploration time in T2 and 8 s of object exploration in T3. Application of this criterion resulted in data analysis from 10 to 13 rats/group. In each group, the cognitive function was ascertained by comparing the percentage of time spent in exploring the object located in the familiar place (familiar place object) with the percentage of time spent in exploring the object moved to a new place (novel place object) in T3. Besides, the total distance traveled, the velocity of movement, and the total object exploration times (TOETs) were measured for both T2 and T3 and compared across groups.

2.5. Measurement of pattern separation function

A pattern separation test (PST), linked to the integrity of the dentate gyrus and the extent of hippocampal neurogenesis, was employed to measure the proficiency of animals for pattern separation, as described in our previous reports [42,43]. The PST comprised four successive trials (T1-T4) with an ITI of 30 min (Fig. 1 [B1]). The trials comprised acclimatization of the animal to the open field apparatus (5 min, T1), exploration of a pair of identical objects placed in distant areas on floor pattern 1 (type 1 objects on pattern 1 or P1; 5 min, T2), exploration of a second pair of identical objects placed in distant areas on floor pattern 2 (type 2 objects on pattern 2 or P2; 5 min, T3), and the exploration of one of the type 2 objects from T3 and one of the type 1 objects from T2 placed on P2 (5 min, T4) (Fig. 1 [B1]). The object from T2 became a new object on P2 (NO on P2), whereas the object retained from T3 was a familiar object on P2 (FO on P2). The movement of the animal in T4 was video-tracked using Anymaze. The data such as times spent in exploring the NO and the FO on P2, the TOET, the velocity, and distance traveled were computed from T4. We set an inclusion criterion that required at least 8 s of object exploration time in T4. Application of this criterion resulted in data analysis from 11 to 14 rats/group. The percentages of object exploration times spent with FO on P2 and NO on P2 were compared within each group. Also, the distance traveled, the velocity of movement, and the TOET in T4 were compared across all groups.

2.6. Characterization of anhedonia or depressive-like behavior

A sucrose preference test (SPT) was used to probe the extent of anhedonia, as described in our previous report [43]. The occurrence of anhedonia in this test is evident from a decreased preference for a sweet fluid such as sucrose or saccharin solution. The test comprised the monitoring of animals for four consecutive days. The rats were housed individually and given free access to two identical bottles containing 1% sucrose solution and were provided ad libitum access to food on day 1. The rats were trained to adapt to the sucrose-containing water for 24 h. One of the bottles was replaced with a new bottle containing regular water and ad libitum access to food on day 2. The animals were deprived of water and food for 22 h on day 3. The animals were tested for their preference towards consuming sucrose-containing water over regular water on day 4 by giving access to two bottles for 2 h, one containing 1% sucrose solution and another containing the regular water. The volumes of liquid consumption in both bottles were measured, and the rats were placed back to their previous housing conditions with ad libitum access to water and food. In each group, the occurrence of anhedonia was assessed by comparing the amount of regular water consumption with the amount of sucrose-containing water consumption.

2.7. Analysis of anxiety-like behavior

A novelty suppressed feeding test (NSFT) was employed to ascertain the degree of anxiety-like behavior, as described in our published report [17]. Following 24-h food deprivation with ad libitum access to water, animals were tested with a single trial lasting 5 min in an open field apparatus to measure the extent of anxiety-like behavior. A small plastic dish containing food was positioned in the middle of the open field equipment, and the animal was let free from one of the sides. The movement of the rat was video-tracked using Anymaze to measure the latency to the first bite of food in seconds, which provided an index of anxiety-like behavior. A higher latency to eat food suggested an enhanced anxiety-like behavior in this test.

2.8. Harvesting of brain tissues and blood

After the completion of behavioral tests (equivalent to 6 months after exposure to GWIR-chemicals and stress in all GWI groups), 5–6 animals from each group were euthanized by decapitation under deep anesthesia as detailed in our previous study [29]. Just before decapitation, the chest cavity was opened from deeply anesthetized animals, and the blood was quickly collected from the right atrium of the heart. The serum was extracted through standard methods and stored at −80°C until further use. The fresh brains from these animals were quickly removed, snap-frozen on dry ice, and stored at −80°C until further analysis. These brain tissues were used for molecular biological and biochemical studies. Furthermore, 7–8 animals from each group were anesthetized and perfused with 4% paraformaldehyde. Animal perfusion and tissue processing protocols such as post-fixation and cryoprotection are detailed in our previous reports [44–46]. These fixed brain tissues were used for various immunohistochemical and immunofluorescence studies.

2.9. Measurement of genes related to oxidative stress via real-time polymerase chain reaction (qRT-PCR)

Following quick thawing, the entire hippocampus from each cerebral hemisphere of the brain was micro-dissected. The hippocampus from one cerebral hemisphere in each animal was chosen for

measurement of the expression of genes that encode proteins relevant for regulating oxidative stress and antioxidant activity, using a qRT-PCR array (n = 4–5/group). The hippocampus from the other cerebral hemisphere and the frontoparietal cortex tissues were used for various biochemical assays. For qRT-PCR studies, the total RNA was extracted using RNeasy kit (Qiagen, Valencia, CA; Cat#: 74104), as described in our previous reports [29,47]. The total RNA (1 μg) was next transcribed to cDNA using the RT2 First Strand Kit (Qiagen, Valencia, CA; Cat# 330404) and stored at −20°C until further analysis, as previously detailed [29,47]. The Rat Oxidative Stress PCR Array employed in this investigation (SABiosciences, Qiagen, Valencia, CA; Cat#: PARN065Z) detected the expression of 84 genes linked to oxidative stress response, ROS metabolism, oxygen transport, and antioxidant activity. A previously described qRT-PCR protocol was employed [47]. The reactions were accomplished as per the manufacturer's protocol using a CFX96 Real-Time System (Bio-Rad, Hercules, CA). The PCR amplification and melt curve analysis were performed as described in our previous report [29]. Next, the Ct (threshold cycle) values from all wells were transferred to an Excel spreadsheet and evaluated using web-based SABiosciences PCR array data analysis software. The 2^delta Ct values for each gene were compared across different groups.

2.10. Measurement of oxidative stress markers from brain tissue lysates and the serum

We measured oxidative stress markers from brain tissue lysates using commercially available kits (n = 5–6/group). The lysates were prepared separately from the frontoparietal cortex and hippocampal tissues, using methods described elsewhere [18,29,48]. Briefly, each brain tissue sample was weighed and lysed in ice-cold tissue extraction buffer (Life Technologies, Carlsbad, CA) with protease inhibitors (Sigma-Aldrich Corp. St. Louis, MO), using a sonic dismembrator for 10 s. The lysed solution was centrifuged twice, and aliquots of the supernatant solution were stored at −80 °C until further use. The protein concentration in different samples was measured using a Pierce BCA reagent kit (Thermo Fisher Scientific, Waltham, MA). We followed manufacturer's instructions that came with the kits for measuring malondialdehyde (MDA, LS-F28018, LSBio, Seattle, WA), 4-hydroxynonenal (4-HNE LS-F40039, LSBio), protein carbonyls (10005020, Cayman Chemical, Ann Arbor, MI), and manganese superoxide dismutase (SOD-2, LS-F6964, LSBio) in samples from all groups. We also measured nuclear factor [erythroid-derived 2]-like 2 (Nrf-2, TE-0027, Signosis, Santa Clara, CA) in the hippocampus of naïve control, GWI-VEH, and GWI-MSL160 groups, as GWI rats receiving 160 mg/kg dose of MSL displayed improvements in all behavioral tests and normalized levels of all three markers of oxidative stress (MDA, 4-HNE and Protein carbonyls). Besides, to examine systemic oxidative stress, we measured MDA and protein carbonyls in serum samples obtained from all groups.

2.11. Immunohistochemistry for glial fibrillary acidic protein (GFAP), ED-1, 5′-bromodeoxyuridine (BrdU), and doublecortin (DCX)

Thirty-micrometer thick coronal sections were cut through the entire hippocampus from fixed brains using a cryocut, collected serially in 24-well plates containing cryobuffer, and stored at −20°C until further analysis. Every 15th or 20th section through the entire septotemporal axis of the hippocampus were processed for immunohistochemical analysis of astrocytes, microglia, and hippocampal neurogenesis (6–8 animals/group). The immunohistochemical studies comprised detection of glial fibrillary acidic protein (GFAP) positive astrocytes, ED-1 positive activated microglia, 5-bromodeoxyuridine (BrdU) positive newly born cells, and doublecortin (DCX) positive newly born neurons. The methods employed are described in our previous reports [17,45,49,50]. The primary antibodies comprised rabbit anti-GFAP (1:1000, Dako, Santa Clara, CA), mouse anti ED-1 (1:1000, Bio-Rad, Hercules, CA), mouse anti-BrdU (1:200, BD, San Jose, CA), and goat polyclonal anti-DCX (1:250; Santa Cruz Biotech, Santa Cruz, CA). The secondary antibodies comprised anti-goat, anti-mouse, or anti-rabbit IgG (Vector Laboratories, Burlingame, CA). The avidin-biotin complex reagent and chromogen kits (vector gray or diaminobenzidine) were obtained from Vector Labs. The sections were next mounted on gelatin-coated slides, dehydrated, cleared, and coverslipped.

2.12. Measurement of hypertrophied astrocytes and ED-1+ activated microglia

The effect of MSL on astrocyte hypertrophy was evaluated by measuring area fractions occupied by GFAP immunoreactive structures in different regions of the hippocampus using Image J (n = 6–8/group) [17,46]. The effect of MSL on microglial activity was investigated by stereological counting of the number of ED-1+ (CD68+) structures through the entire hippocampus in serial sections (every 20th) from GWI-VEH and GWI-MSL groups (n = 8/group), as described in our previous reports [45,48]. Furthermore, the effect of MSL for reducing the occurrence of activated microglia was ascertained through IBA-1 and ED-1 dual immunofluorescence with Z-section analyses in a confocal microscope, as described in our previous studies [18]. The primary antibodies employed were goat anti-IBA-1 (1:1000, Abcam, Cambridge, MA) and mouse ED-1 (1:1000, Bio-Rad), and secondary antibodies used were donkey anti-mouse IgG tagged with Alexa Fluor 594 (1:200, Thermo Fisher Scientific) and donkey anti-goat IgG tagged with Alexa Flour 488 (1:200, Thermo Fisher Scientific). The sections were coverslipped with a slow fade/antifade mounting medium (Thermo Fisher Scientific). Percentages of IBA-1+ cells that expressed ED-1 were then quantified by examination of individual IBA-1+ cells in 1.5-μm thick optical Z-sections. The percentages of activated microglia (ED-1+) among all microglia (IBA-1+) were computed and compared between GWI-VEH and GWI-MSL groups (n = 6/group).

2.13. Quantification of hippocampal neurogenesis

The numbers of new cells that were born in the third week of MSL or VEH treatment and survived for five weeks were measured via stereological counting of $BrdU^+$ cells in the subgranular zone-granule cell layer (SGZ-GCL) of the dentate gyrus. The status of hippocampal neurogenesis at the time of euthanasia (equivalent to ~6 months after exposure to GWIR-chemicals and stress and after two months of MSL or VEH treatment) was measured through stereological quantification of DCX positive newly born neurons in the SGZ-GCL of the dentate gyrus. The stereological method for BrdU+ and DCX + cell counts utilized every 15th section through the entire hippocampus (n = 6–8/group), as detailed in our previous reports [51,52]. Furthermore, BrdU and neuron-specific nuclear antigen (NeuN) dual immunofluorescence and Z-section analyses in a Nikon confocal microscope were employed to quantify the extent of neuronal differentiation of newly born cells and net neurogenesis, as described in our previous report [49]. The primary and secondary antibodies comprised mouse anti-NeuN (1:1000, EMD Millipore, Temecula, CA), rat anti-BrdU (1:250, Serotech), donkey anti-mouse IgG tagged with Alexa Flour 488 (1:200, Invitrogen, Grand Island, NY), and donkey anti-rat IgG tagged with Alexa Flour 594 (1:200, Invitrogen). Percentages of BrdU + cells that expressed NeuN were then quantified by examination of individual BrdU + cells in 1-μm thick optical Z-sections.

2.14. Measurement of cytokines and chemokines in the serum

We employed a quick and sensitive rat cytokine array to estimate 16 cytokines/chemokines in the serum, as per manufacturer instructions (Signosis; Cat#: EA4006) and as described in our previous report [29]. The values for each biomarker were compared across groups (n = 6/group).

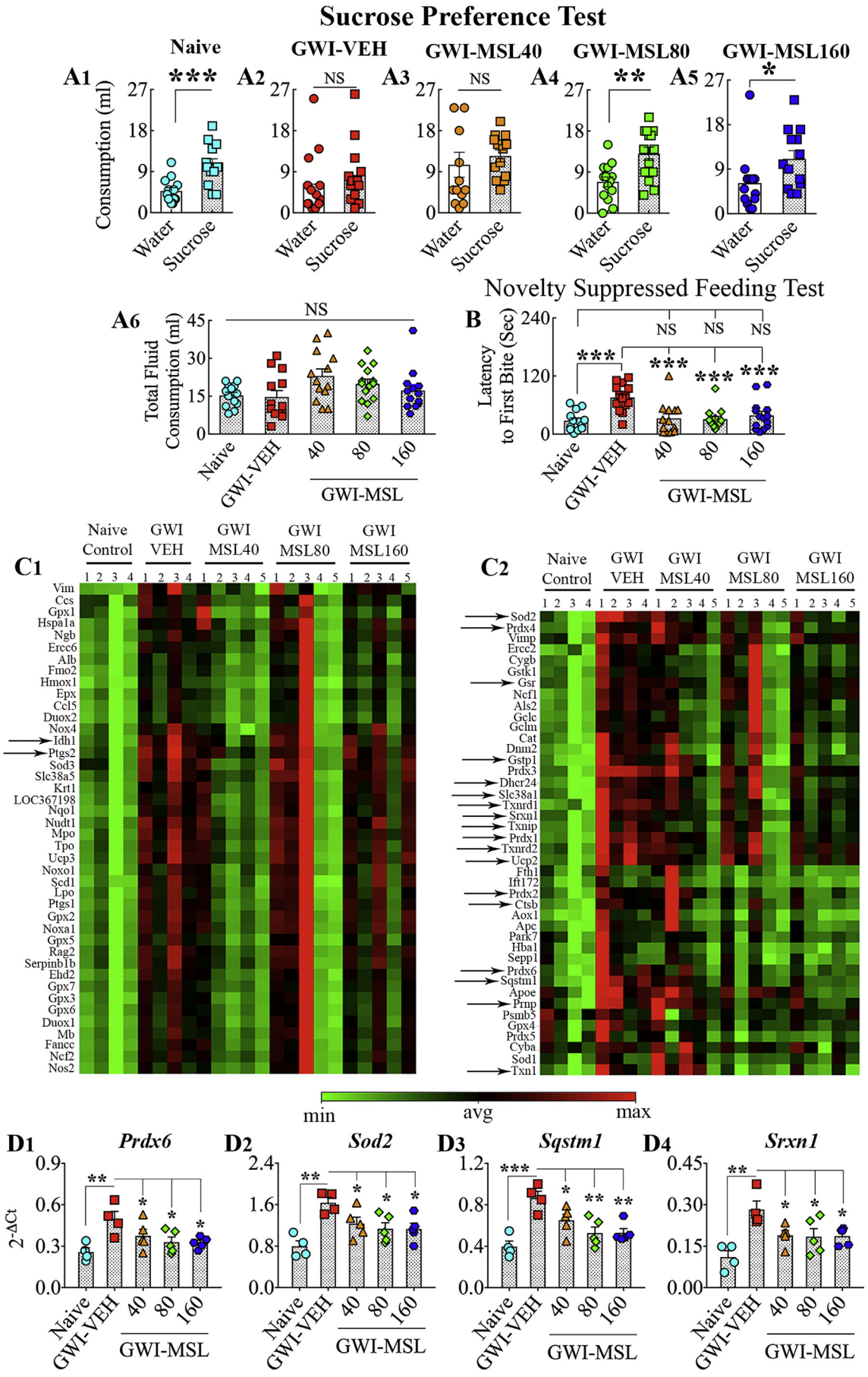

(caption on next page)

Fig. 2. A1-B: Monosodium Luminol (MSL) treatment to rats with Gulf War Illness (i.e., GWI rats) reduced their depressive- and anxiety-like behavior. The bar charts in A1-A5 illustrate the performance of animals belonging to naïve control (Naive, A1), GWI animals receiving vehicle (GWI-VEH, A2), and GWI animals receiving different doses of MSL (GWI-MSL40, GWI-MSL80, GWI-MSL160; A3-A5) in a sucrose preference test, which is a test for measuring anhedonia or depressive-like behavior. Animals belonging to GWI-VEH (A2) and GWI-MSL40 groups were impaired (A3), which was evident from their lack of preference for the sucrose-containing water over the regular water. In contrast, animals in naïve (A1), GWI-MSL80 (A4), and GWI-MSL160 (A5) groups consumed a greater amount of sucrose-containing water than the regular water, implying no anhedonia. The bar chart in A6 compares the total fluid consumption across groups. The bar chart in B compares latencies to the first bite of food in a novelty suppressed feeding test between different groups of animals. Note that animals belonging to the GWI-VEH group displayed higher latencies to eat food than rats in the naïve control group, implying the presence of anxiety-like behavior in these rats. In contrast, animals in GWI-MSL groups exhibited comparable latencies to eat food as naïve control animals suggesting reduced anxiety. *, $p < 0.05$, **, $p < 0.01$, ***, and $p < 0.001$; NS, not significant. **C1-D4:** MSL treatment to GWI rats normalized the expression of multiple genes encoding proteins that combat oxidative stress. Figures C1 and C2 are cluster diagrams comparing the relative expression of various genes between animals belonging to naive, GWI-VEH, and GWI-MSL groups. Arrows in C1–C2 denote genes that displayed increased expression in the GWI-VEH group but normalized to levels in the naïve control group in one or more of MSL treated groups. The bar charts in D1-D4 illustrate the expression of 4 genes *(Prdx6, Sod2, Sqstm1, Srxn1)* that were reduced by all doses of MSL treatment. *, $p < 0.05$, **, $p < 0.01$, and ***, $p < 0.001$.

2.15. Statistical analyses

We employed two-tailed, unpaired, Student's t-test for analyses of data within groups, and one-way ANOVA with Newman-Keuls multiple comparison post-tests for comparison of data across all groups.

3. Results

3.1. MSL treatment improved object location memory in GWI rats

The object location memory (OLM) task measures cognitive function, mainly spatial memory, and the ability to recognize minor changes in the immediate environment. Proficiency in this task relies heavily on hippocampal activity, particularly the dorsal CA1 region [28]. The hippocampus provides a cognitive map of the organism's immediate environment and stores information about spatial relationships between objects and places in the area. Naïve control animals showed a proclivity to inspect the object repositioned to a new location in OLT, which confirmed their competence for this task ($t = 4.2$, $p < 0.001$, Fig. 1 [A1-A2]). In contrast, animals belonging to the GWI-VEH group exhibited OLM dysfunction, which was evident from their exploration of the familiar place object (FPO) and the novel place object (NPO) for comparable durations ($t = 1.4$, $p > 0.05$, Fig. 1 [A3]). Interestingly, GWI animals receiving different doses of MSL demonstrated similar behavior as naïve control animals, as they explored a significantly higher amount of their object exploration time with the NPO ($t = 2.04–5.3$, $p = 0.05$ or $< 0.01–0.0001$, Fig. 1 [A4-A6]). The total distance traveled, the velocity of movement, and the total object exploration times (TOETs) in the sample trial (T2) were comparable across the five groups ($F = 0.5–1.5$, $p > 0.05$, Fig. 1 [A7-A9]), implying that the test results were not influenced by different levels of object exploration or motor deficits in one or more groups. These parameters were also comparable between groups in T3 ($F = 1.4–1.7$, $p > 0.05$), and the TOETs in different groups for T3 are illustrated (Fig. 1 [A10]). Thus, eight weeks of MSL treatment to GWI rats at 40–160 mg/kg improved hippocampus-dependent cognitive function.

3.2. MSL treatment at a higher dose improved pattern separation function in GWI rats

We interrogated the cognitive ability of GWI rats in different groups through a PST. The ability to differentiate similar but not identical experiences is a critical feature of episodic memory [53]. Pattern separation ability is critical for successfully recalling such overlapping experiences, which is a competence for discriminating similar experiences via the storage of representations in a non-overlapping manner [53]. Excellent pattern separation ability in naïve control rats was revealed by exploration of the object from T2 (i.e., novel object on pattern 2 [NO on P2]) for longer durations than the object from T3 (i.e., the familiar object on pattern 2 [FO on P2] ($t = 6.7$, $p < 0.0001$, Fig. 1 [B1–B2]). GWI rats that received VEH (GWI-VEH) showed no preference for the NO on P2 however, as they spent nearly similar amounts of their object exploration time with the NO and the FO on P2 ($t = 0.02$, $p > 0.05$, Fig. 1 [B3]), implying the loss of ability for pattern separation with GWI. GWI rats that received lower doses of MSL-GVT (40–80 mg/kg) also remained impaired, which was evident from either exploration of the FO on P2 for more extended periods than the NO on P2 ($t = 2.3$, $p < 0.05$, Fig. 1 [B4]) or exploration of the FO and NO for comparable durations ($t = 0.7$, $p > 0.05$, Fig. 1 [B5]). In divergence, GWI rats that received higher doses of MSL-GVT (160 mg/kg) displayed ability for pattern separation, which was apparent from their exploration of the NO on P2 for longer durations than the FO on P2 ($t = 2.1$, $p < 0.05$, Fig. 1 [B6]). No differences were seen for the total distance traveled, the velocity of movement, and the TOET between groups ($F = 1.5–2.0$, $p > 0.05$, Fig. 1 [B7–B9]), which confirmed that the outcomes were not influenced by varying object exploration times or motor deficits in one or more groups. Thus, lower doses of MSL-GVT were not efficacious for reversing pattern separation dysfunction. However, cognitive impairment related to pattern separation could be improved in GWI rats through the administration of MSL at a higher dose.

3.3. MSL treatment improved mood function in GWI rats

GWI is also characterized by mood impairment. Therefore, we measured the extent of anhedonia in naïve control and different groups of GWI rats using a sucrose preference test. Anhedonia is a condition of decreased ability to perceive pleasure in activities that are pleasurable in normal healthy conditions, which is a common symptom of depression. The sucrose preference test provides a measure of anhedonia in rodents by their preference for drinking sweet fluids over regular water. Naive control animals did not display anhedonia in this test, as they drank a higher volume of sucrose-containing water than regular water ($t = 4.0$, $p < 0.001$, Fig. 2 [A1]). On the other hand, GWI rats receiving vehicle or 40 mg/kg MSL demonstrated the presence of anhedonia by consuming comparable volumes of regular water and sucrose-containing water ($t = 0.6–0.7$, $p > 0.05$, Fig. 2 [A2-A3]). In contrast, GWI rats receiving higher doses of MSL (80–160 mg/kg) exhibited a behavior akin to naïve control animals by consuming a higher volume of sucrose-containing water than regular water ($t = 2.1–3.4$, $p < 0.05–0.01$, Fig. 2 [A4-A5]), which implied no anhedonia in these animals. The overall fluid consumption (i.e., sucrose-containing water + regular water) in the testing period was comparable across the five groups ($F = 2.4$, $p > 0.05$, Fig. 2 [A6]), which confirmed that differences in the total fluid consumption by one or more groups did not influence the results.

3.4. MSL treatment reduced anxiety-like behavior in GWI rats

Anxiety-like behavior in naïve control and different groups of GWI rats was measured using a novelty suppressed feeding test (NSFT). In this test, the latency to eat a familiar food in a new environment

provides a measure of anxiety, as animals will require to settle a struggle between a situation that engenders increased anxiety and the motive to reach an appetitive stimulus [54]. Animals with anxiety typically take longer times to reach and eat food than animals having no anxiety. A comparison of latencies to the first bite using one-way ANOVA revealed differences in anxiety levels between groups ($F = 7.3$, $p < 0.0001$, Fig. 2 [B]). Naïve control animals did not exhibit anxiety-like behavior, as their latency values to reach and take the first bite of food were minimal (Fig. 2 [B]). GWI rats demonstrated anxiety-like behavior by taking a considerably higher amount of time to eat food than naïve control rats ($p < 0.001$). In contrast, latencies to eat food in GWI rats receiving different doses of MSL were comparable to naïve control rats ($p > 0.05$) and significantly lower than GWI rats receiving vehicle ($p < 0.001$, Fig. 2 [B]). Thus, MSL treatment reduced anxiety-like behavior in GWI rats at all doses examined in this study.

3.5. MSL treatment to GWI rats normalized the expression of multiple genes encoding proteins involved in combating oxidative stress

We examined the expression of 84 genes implicated in oxidative stress response and antioxidant activity in the hippocampus of different groups using qRT- PCR (Fig. 2 [C1–C2]). GWI rats receiving VEH displayed enhanced expression of multiple genes, in comparison to age-matched naive control animals (Fig. 2 [C1–C2]), which suggested the occurrence of significant oxidative stress in the brain of GWI rats, as noted in our previous study [29]. However, in GWI rats receiving MSL, the expression of many of these genes was closer to naïve control animals and reduced in comparison to GWI rats receiving VEH. Notably, ANOVA analyses demonstrated that all doses of MSL treatment reduced the expression of 4 genes ($F = 6.0–9.1$, $p < 0.05–0.001$, Fig. 2[D1-D4]). The genes include *Prdx6, Sod2, Sqstm1, and Srxn1* (Fig. 2 [D1-D4]). These genes respectively encode proteins peroxiredoxin-6, mitochondrial manganese-dependent SOD-2 (MnSOD), sequestosome 1 or p62, and sulforedoxin-1. Furthermore, higher doses of MSL modulated the expression of 16 genes that displayed increased expression in GWI rats receiving vehicle (Fig. 2 [C1–C2], Table 1). When compared with age-matched naïve control animals, the expression of these genes was higher in GWI rats receiving VEH ($p < 0.05–0.01$) but not in GWI rats receiving higher doses of MSL-GVT ($p > 0.05$, Table 1). These genes encode proteins, cathepsin B (*Ctsb*), 24-dehydrocholesterol reductase (*Dhcr24*), glutathione reductase (*Gsr*), glutathione s-transferase-1 (*Gstp1*), isocitrate dehydrogenase 1 (*Idh1*), peroxiredoxin (*Prdx)1, 2 and 4*, prion protein (*Prnp*), prostaglandin-endoperoxide synthase or cyclooxygenase (*Ptgs2*), solute carrier family 38, member 1 protein (*Slc38a1*), thioredoxin 1 (*Txn1*), thioredoxin interacting protein (*Txnip*), thioredoxin reductase protein 1-2 (*Txnrd1-2*) and uncoupling protein 2 (*Ucp2*). The function of proteins encoded by these genes is detailed in Table 1. Overall, these studies on genes related to oxidative stress suggested that MSL treatment at higher doses improves redox balance in the brain of GWI rats.

3.6. MSL treatment at a higher dose reinstated redox homeostasis in the brain of GWI rats

We quantified several markers of oxidative stress in the brain, which comprised MDA, 4-HNE, and PCs. Analyses using ANOVA revealed differences between groups for all three markers ($F = 6.5–11.3$, $p < 0.01–0.0001$, Fig. 3 [A1-A3]). In comparison to the brain of naïve control animals, the brain of GWI rats receiving vehicle exhibited higher concentrations of MDA ($p < 0.001$, Fig. 3 [A1]), 4-HNE ($p < 0.01$, Fig. 3 [A2]) and PCs ($p < 0.05$, Fig. 3 (A3]), confirming a state of impaired redox homeostasis in the brain of GWI rats. In GWI rats receiving 40 mg/kg MSL, MDA and 4-HNE levels remained similar to GWI rats receiving vehicle ($p > 0.05$) but the level of PCs was less than that seen in GWI rats receiving vehicle ($p < 0.05$, Fig. 3 [A3]), which suggested reduced protein oxidation in GWI rats receiving 40 mg/kg MSL. In the brain of GWI rats receiving 80 mg/kg MSL, MDA concentration remained as high as GWI rats receiving vehicle ($p > 0.05$, Fig. 3 [A1]) but concentrations of 4-HNE and PCs were less than that observed in GWI rats receiving vehicle ($p < 0.05–0.001$, Fig. 3 [A2-A3]), which implied that 80 mg/kg MSL treatment reduced lipid peroxidation and normalized protein oxidation in GWI rats. However, the most beneficial effects of MSL treatment were seen when 160 mg/kg dose was employed in GWI rats. In these GWI rats, MDA, 4-HNE, and PC levels in the brain were less than that seen in GWI rats receiving vehicle ($p < 0.05–0.0001$, Fig. 3 [A1-A3]). Also, MDA and 4-HNE levels were normalized to naïve control levels ($p > 0.05$, Fig. 3 [A1-A2]), and the concentration of PCs went lower than the concentration seen in naïve control animals ($p < 0.05$, Fig. 3 [A3]). Thus, 160 mg/kg MSL treatment reinstated redox homeostasis in the brain of GWI rats.

We next investigated whether changes mediated by MSL affected the innate response of the organism to combat oxidative stress. For this, we measured concentrations of SOD-2 and NRF-2 in the hippocampus. SOD-2 is a mitochondrial antioxidant, whereas NRF-2 is a transcription factor involved in the regulation of oxidative stress. Both of these markers are typically upregulated in conditions of increased oxidative stress. ANOVA analysis revealed differences between groups for both SOD-2 and NRF-2 ($F = 7.9–84.1$, $p < 0.01–0.0001$, Fig. 3 [B1–B2]). In comparison to naïve control animals, the brain of GWI rats receiving vehicle displayed increased levels of SOD-2 ($p < 0.01$, Fig. 3 [B1]) and NRF-2 ($p < 0.001$, Fig. 3 [B2]). However, MSL treatment to GWI rats did not alter the concentration of SOD-2 ($p < 0.01$ to 0.001) or NRF-2 ($p < 0.001$) in the brain. Thus, MSL treatment reinstated redox homeostasis in the brain of GWI rats without altering the brain's innate defense mechanisms against increased oxidative stress, which is apparent from increased concentrations of SOD-2 and NRF-2.

3.7. MSL treatment at a higher dose also reduced systemic oxidative stress in GWI rats

Because eight weeks of oral administration of MSL at a higher dose reinstated redox homeostasis in the brain, we wondered whether such treatment also reduced oxidative stress at the systemic level. We quantified the concentrations of MDA and PCs in the serum of all groups of rats. Evaluation using ANOVA demonstrated significant differences between groups ($F = 13.9–26.8$, $p < 0.0001$, Fig. 3 [C1, C2]). In comparison to the serum from naïve control rats, the serum of GWI rats displayed elevated levels of both MDA and PCs ($p < 0.0001$, Fig. 3 [C1, C2]). GWI rats receiving MSL at 40 or 80 mg/kg did not display reduced MDA levels in the serum ($p > 0.05$ in comparison to GWI rats receiving vehicle and $p < 0.0001$ in comparison to naïve control animals, Fig. 3 [C1]). However, GWI rats receiving 160 mg/kg MSL demonstrated reduced MDA concentration than GWI rats receiving vehicle ($p < 0.0001$ Fig. 3 [C1]) though the overall concentration remained higher than that seen in naïve control animals ($p < 0.05$, Fig. 3 [C1]). The concentration of PCs, on the other hand, were reduced in GWI rats with all doses of MSL tested in the study ($p < 0.01$ in comparison to GWI rats receiving vehicle and $p > 0.05$ in comparison to naïve control animals, Fig. 3 [C2]).

3.8. MSL treatment to GWI rats reduced hypertrophy in astrocytes

We quantified astrocyte hypertrophy to gauge the extent of neuroinflammation in GWI rats receiving vehicle or MSL. The morphology of GFAP + astrocytes in the DG, the CA1 subfield, and the CA3 subfield of the hippocampus are illustrated in Fig. 4. In comparison to naïve control animals (Fig. 4 [A1-A3]), the presence of hypertrophied astrocytes was conspicuously seen in GWI rats receiving the vehicle (Fig. 4 [B1–B3]). However, the overall hypertrophy seemed to be reduced in GWI rats receiving MSL, with most reductions apparent in GWI rats receiving 160 mg/kg dose of MSL (Fig. 4, C1–C3, D1-D3, E1-E3]).

Table 1
Genes that displayed increased expression in GWI rats but normalized to naïve control levels after MSL-GVT treatment. (ANOVA: $p < 0.05–0.01$; $F = 3.0–4.7$).

Gene	Description	Function	Differences between groups (post hoc test)s
Ctsb	Cathepsin B	Involved in the proteolytic processing of amyloid precursor protein	Naïve versus GWI, $p < 0.05$; Naïve versus MSL40, MSL80 or MSL160, $p > 0.05$.
Dhcr24	24-Dehydrocholesterol Reductase	A oxidoreductase, involved in cholesterol biosynthesis	Naïve versus GWI, $p < 0.05$; Naïve versus MSL40, MSL80 or MSL160, $p > 0.05$.
Gsr	Glutathione-Disulfide Reductase	Reduces oxidized glutathione disulfide to the sulfhydryl form GSH	Naïve versus GWI, $p < 0.05$; Naïve versus MSL40, MSL80 or MSL160, $p > 0.05$.
Gstp1	Glutathione S-Transferase Pi 1	Involved in detoxification by catalyzing the conjugation of many hydrophobic and electrophilic compounds with reduced glutathione	Naïve versus GWI, $p < 0.05$; Naïve versus MSL40, MSL80 or MSL160, $p > 0.05$.
Idh1	Isocitrate Dehydrogenase (NADP(+)) 1, Cytosolic	Converts isocitrate to 2- ketoglutarate to produce NADPH necessary for many cellular processes and protection against ROS	Naïve versus GWI, $p < 0.05$; Naïve versus MSL40, MSL80 or MSL160, $p > 0.05$.
Prdx1, 2, and 4	Peroxiredoxins 1, 2 and 4	Antioxidant enzymes involved in reducing hydrogen peroxide and alkyl hydroperoxides to water and alcohol with the use of reducing equivalents derived from thiol-containing donor molecules	Naïve versus GWI, $p < 0.05–0.01$; ***Prdx1:*** Naïve versus MSL40, MSL80 or MSL160, $p > 0.05$. ***Prdx2:*** Naïve versus MSL40, $p < 0.05$; Naïve versus MSL80 or MSL160, $p > 0.05$. ***Prdx4:*** Naïve versus MSL40, $p < 0.05$; Naïve versus MSL80 or MSL160, $p > 0.05$.
Prnp	Prion Protein	Membrane glycosylphosphatidylinositol-anchored glycoprotein that tends to aggregate into rod-like structures.	Naïve versus GWI, $p < 0.05$; Naïve versus MSL40, $p < 0.05$; Naïve versus MSL80 or MSL160, $p > 0.05$.
Ptgs2	Prostaglandin-Endoperoxide Synthase 2	A key enzyme in prostaglandin biosynthesis, and acts both as a dioxygenase and as a peroxidase	Naïve versus GWI, $p < 0.05$; Naïve versus MSL40, MSL80 or MSL160, $p > 0.05$.
Slc38a1	Solute Carrier Family 38 Member 1	An important transporter of glutamine, an intermediate in the detoxification of ammonia and the production of urea	Naïve versus GWI, $p < 0.05$; Naïve versus MSL40, MSL80 or MSL160, $p > 0.05$.
Txn1	Thioredoxin	Participates in various redox reactions through the reversible oxidation of its active center dithiol to a disulfide and catalyzes dithiol- disulfide exchange reactions	Naïve versus GWI, $p < 0.05$; Naïve versus MSL40, MSL80 or MSL160, $p > 0.05$.
Txnip	Thioredoxin Interacting Protein	Act as an oxidative stress mediator by inhibiting thioredoxin activity or by limiting its bioavailability	Naïve versus GWI, $p < 0.05$; Naïve versus MSL40, MSL80 or MSL160, $p > 0.05$.
Txnrd1	Thioredoxin Reductase 1	Reduces thioredoxins as well as other substrates, and plays a role in selenium metabolism and protection against oxidative stress.	Naïve versus GWI, $p < 0.05$; Naïve versus MSL40, MSL80 or MSL160, $p > 0.05$.
Txnrd2	Thioredoxin Reductase 2	Maintains thioredoxins in a reduced state, and thereby plays a key role in regulating the cellular redox environment.	Naïve versus GWI, $p < 0.05$; Naïve versus MSL40, MSL80 or MSL160, $p > 0.05$.
Ucp2	Uncoupling Protein 2	Facilitates the transfer of anions from the inner to the outer mitochondrial membrane and the return transfer of protons from the outer to the inner mitochondrial membrane	Naïve versus GWI, $p < 0.01$; Naïve versus MSL40, MSL80 or MSL160, $p > 0.05$.

The function of various genes mentioned above was obtained from GeneCards (human gene database at: http://www.genecards.org), National Center for Biotechnology Information (NCBI at: http://www.ncbi.nlm.nih.gov/gene)and Online Mendelian Inheritance in Man (OMIM at: http://www.omim.org).

Quantification and comparison of the area fraction of GFAP + astrocytes using ANOVA revealed significant differences between groups ($F = 5.7–29.7$, $p < 0.01–0.0001$, Fig. 4 [F1–F4]). Increased density of GFAP + astrocytic elements was seen in all subfields of the hippocampus of GWI rats receiving the vehicle, in comparison to naïve control animals ($p < 0.01–0.0001$, Fig. 4 [F1–F4]). Next, we compared the extent of astrocyte hypertrophy between GWI rats receiving vehicle and GWI rats receiving different doses of MSL. GWI rats receiving 40 mg/kg MSL exhibited a reduced density of GFAP + astrocytic elements in the DG and when the hippocampus was measured in its entirety ($p < 0.05–0.01$, Fig. 4 [F1, F4]). GWI rats receiving 80 mg/kg MSL exhibited a reduced density of GFAP + structures in the DG, the CA1 subfield, and when the hippocampus was measured in its entirety ($p < 0.001–0.0001$, Fig. 4 [F1, F2, F4]). GWI rats receiving 160 mg/kg MSL exhibited a reduced density of GFAP + elements in all subfields of the hippocampus ($p < 0.05–0.0001$, Fig. 4 [F1–F4]). Also, the extent of astrocytic elements in these rats was comparable to levels seen in naïve control animals for all measured regions ($p > 0.05$, Fig. 4 [F1–F3]). Thus, MSL treatment at a higher dose reversed astrocyte hypertrophy in GWI rats.

3.9. MSL treatment modulated the phenotype of microglia from reactive to a resting type

We investigated the occurrence and the extent of activated microglia in the cerebral cortex and the hippocampus of GWI rats (Fig. 5 [A1-O]). Activated microglia were conspicuous in the brain of GWI rats receiving vehicle by their expression of markers IBA-1 and ED-1 (CD68), and hypertrophied soma with less ramified processes (Fig. 5 [B1–B3, G1-G3]). The density of such activated microglia did not appear to change significantly in GWI rats receiving 40 or 80 mg/kg MSL (Fig. 5 [C1–C3, D1-D3, H1–H3, I1–I3]) but reduced in GWI rats receiving 160 mg/kg MSL (Fig. 5 [E1-E3, J1-J3]). Quantification of the percentages of ED-1+ cells among IBA-1+ cells confirmed the

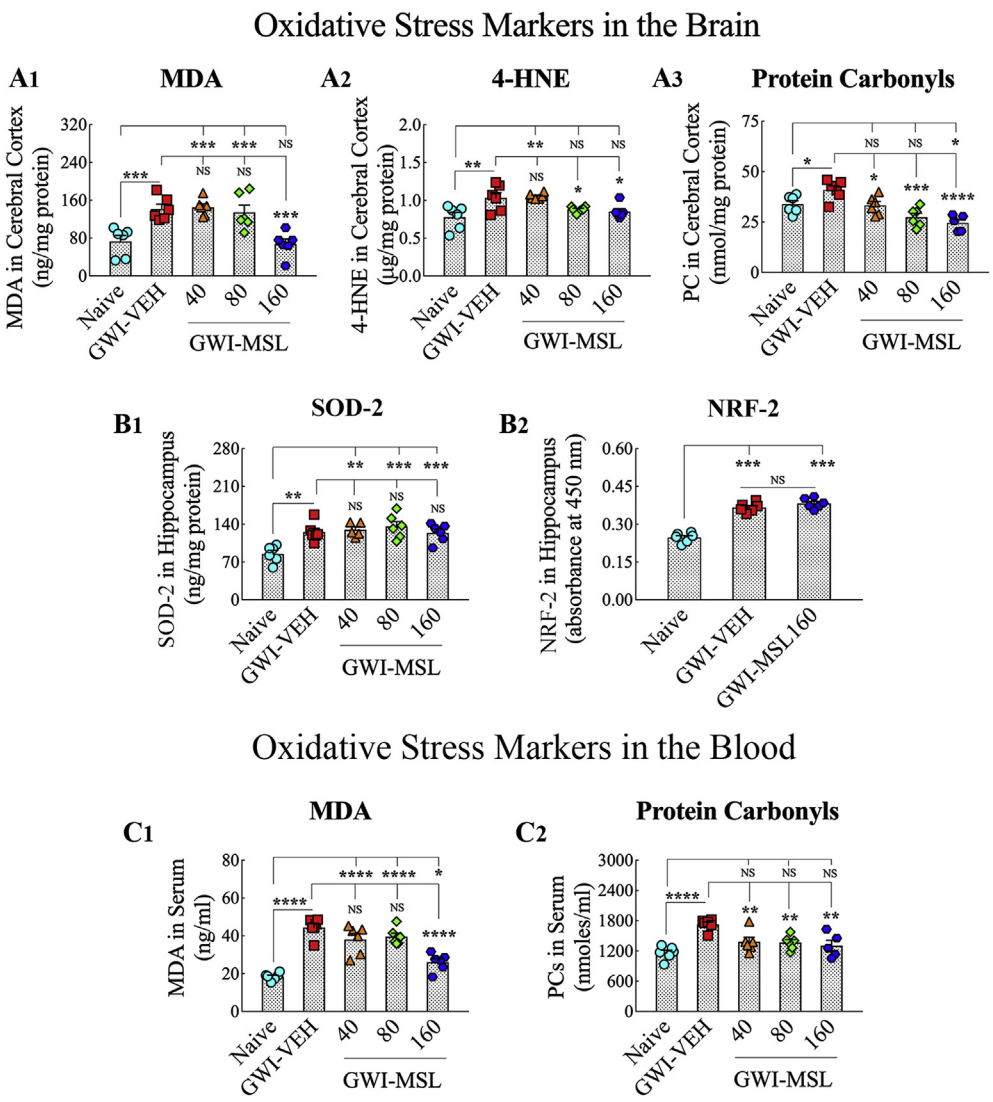

Fig. 3. Monosodium Luminal (MSL) treatment to rats with Gulf War Illness (i.e., GWI rats) normalized the expression of several markers of oxidative stress in the brain and the blood. The bar charts in A1-A3 compare the concentration of malondialdehyde (MDA), 4-hydroxynonenal (4-HNE), and protein carbonyls (PCs) in the cerebral cortex of naïve, GWI rats receiving vehicle (GWI-VEH) and GWI rats receiving different doses of MSL (GWI-MSL40, GWI-MSL80, GWI-MSL160). Note that, concentrations of all three markers were upregulated in animals belonging to the GWI-VEH group, in comparison to the naïve control group. In contrast, GWI rats receiving MSL (particularly higher doses of MSL) displayed concentrations that are comparable to the naïve control group. The bar charts in B1–B2 compare the concentration of superoxide dismutase-2 (Sod-2) and Nrf-2 in the hippocampus of animals belonging to different groups. Note that, in comparison to naïve controls, animals in the GWI-VEH group displayed increased levels of Sod2 and Nrf-2, but MSL treatment did not alter their concentration. The bar charts in C1–C2 compare the concentration of MDA and PCs in the serum of animals belonging to different groups. Note that animals in the GWI-VEH group displayed elevated levels of MDA and PCs in the serum. Also, MSL treatment at 160 mg/kg reduced MDA concentration, and all doses of MSL treatment reduced the concentration of PCs in GWI rats. *, $p < 0.05$, **, $p < 0.01$, ***,$p < 0.001$, and ****, $p < 0.0001$; NS, not significant.

transformation of > 50% of microglia into an activated phenotype in the cerebral cortex and the DG, CA1, and CA3 subfields of the hippocampus in GWI rats receiving vehicle (Fig. 5 [K–O]). Next, we compared percentages of activated microglia between GWI rats receiving vehicle and GWI rats receiving different doses of MSL using ANOVA, which revealed significant differences between groups for the cerebral cortex, CA1 and CA3 subfields and the entire hippocampus ($F = 5.3–9.5$, $p < 0.01–0.001$, Fig. 5 [K, M − O]). MSL treatment at 40 or 80 mg/kg to GWI rats did not reduce the percentages of activated microglia in most regions. The only exception was when the hippocampus was measured in its entirety ($p < 0.05$, Fig. 5 [O]). However, MSL treatment at 160 mg/kg to GWI rats reduced percentages of activated microglia in the cerebral cortex, the CA1 and CA3 subfields, and the entire hippocampus ($p < 0.01–0.001$, Fig. 5 [K, M − O]). We also confirmed the reduced occurrence of activated microglia in GWI rats receiving a higher dose of MSL through stereological counting of ED-1+ structures in the entire hippocampus (see Supplemental Fig. 1). Thus, MSL treatment at a higher dose reduced the density of activated microglia, suggesting that reinstatement of redox homeostasis by MSL altered the phenotype of a significant percentage of microglia from reactive to a resting type.

3.10. Three weeks of MSL treatment did not improve neurogenesis in GWI rats

We quantified hippocampal neurogenesis through in vivo BrdU labeling for five days in the 3rd week of vehicle or MSL treatment. Quantification of BrdU + cells and fractions of BrdU + cells expressing the mature neuronal marker NeuN in the SGZ-GCL facilitated the quantification of net hippocampal neurogenesis (See Supplemental Fig. 2). Quantification of BrdU labeled cells demonstrated decreased production of newly born cells in the SGZ-GCL of GWI rats receiving the vehicle in comparison to naive control rats (Supplemental Fig. 2). However, three weeks of MSL treatment did not enhance the production of new cells, as GWI rats treated with all doses of MSL exhibited BrdU + cell numbers that were comparable to GWI rats receiving the vehicle. Quantification of the neuronal differentiation of newly born cells demonstrated a similar extent of conversion of newly born cells into neurons in all groups (Supplemental Fig. 2). Measurement of net hippocampal neurogenesis (using BrdU + cell numbers and percentages of neuronal differentiation of BrdU + cells) revealed decreased neurogenesis in GWI rats receiving the vehicle and GWI rats receiving different doses of MSL, in comparison to age-matched naive control rats (Supplemental Fig. 2). Thus, MSL treatment for a shorter duration (3 weeks) is not efficient for enhancing hippocampal neurogenesis in GWI rats.

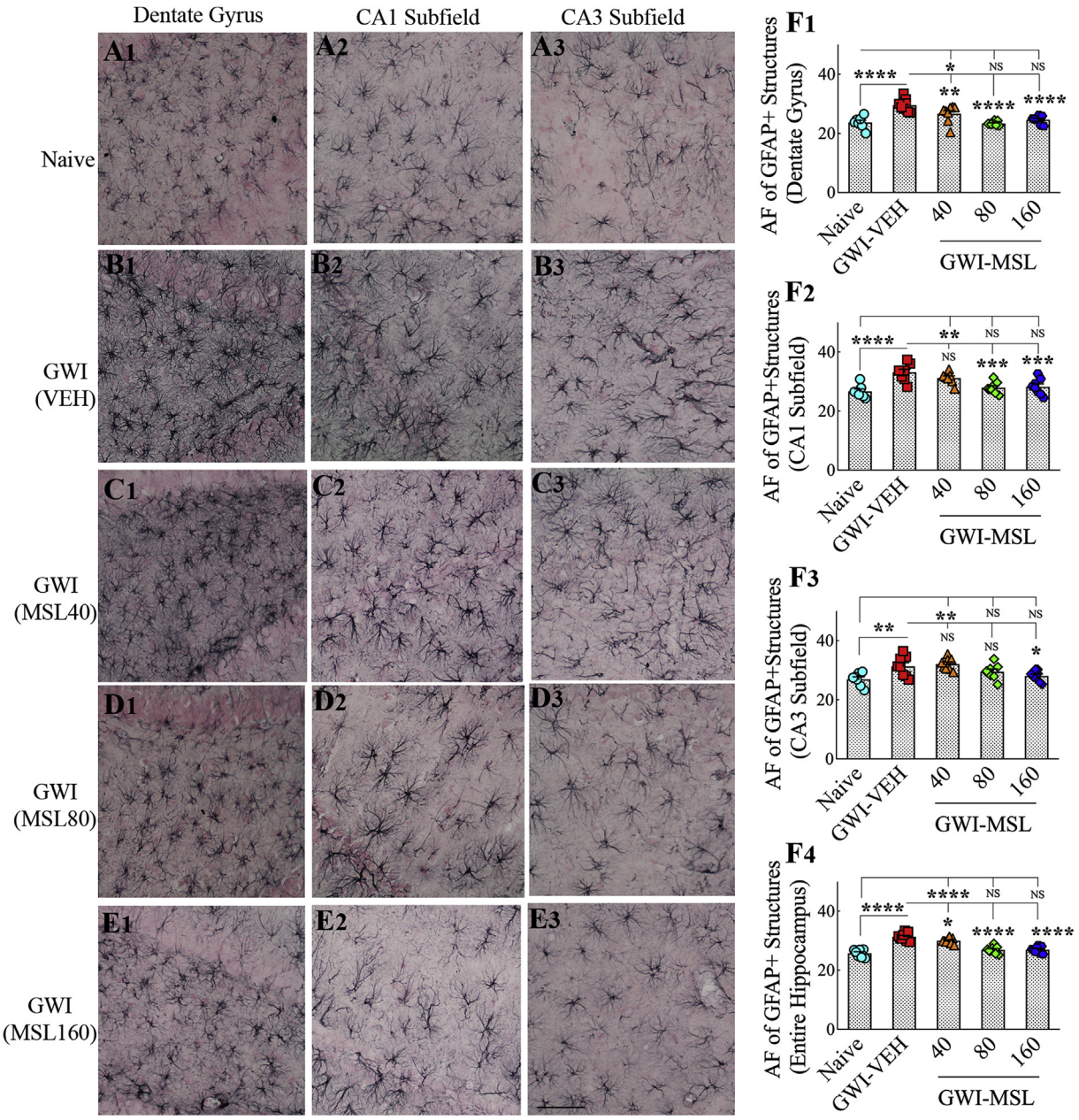

Fig. 4. Monosodium Luminal (MSL) treatment to rats with Gulf War Illness (i.e., GWI rats) reduced astrocyte hypertrophy in the brain. A1-E3 show the distribution and morphology of GFAP + astrocytes in the dentate gyrus (DG; A1, B1, C1, D1, E1), the CA1 subfield (A2, B2, C2, D2, E2) and the CA3 subfield (A3, B3, C3, D3, E3) from a naïve control animal (A1-A3), a GWI rat receiving vehicle (GWI-VEH, B1–B3) and GWI animals receiving different doses of MSL (GWI-MSL40, C1–C3; GWI-MSL80, D1-D3; GWI-MSL160; E1-E3). The bar charts in F1–F4 compare the area fraction (AF) of GFAP + structures in the DG (F1), the CA1 subfield (F2), the CA3 subfield (F3), and the entire hippocampus (F4) between different groups. Note that GWI rats receiving 160 mg/kg MSL exhibited a reduced density of GFAP + elements in all subfields of the hippocampus. *, $p < 0.05$, **, $p < 0.01$, and ****, $p < 0.0001$; NS, not significant. Scale bar, A1-E3 = 100 μm.

3.11. Eight weeks of MSL treatment normalized hippocampal neurogenesis in GWI rats

We examined newly born neurons and quantified their numbers in the SGZ-GCL of the hippocampus using DCX immunostaining, which provided information on the status of hippocampal neurogenesis at the end of eight weeks of the vehicle or MSL treatment (Fig. 6 [A1-E2, F]). Analysis using ANOVA revealed significant differences between groups ($F = 6.6$, $p < 0.001$). Decreased production of newly born neurons in the SGZ-GCL of the hippocampus was observed in GWI rats receiving the vehicle, in comparison to age-matched naive control rats ($p < 0.001$, Fig. 6 [A1-B2, F]). Next, we compared the numbers of DCX + newly born neurons between GWI rats receiving vehicle and GWI rats receiving different doses of MSL. Treatment of GWI rats at 40 mg/kg MSL did not improve neurogenesis in the hippocampus ($p > 0.05$ in comparison to GWI rats receiving the vehicle, Fig. 6 [B1–C2, F]). Treatment of GWI rats at 80 or 160 mg/kg MSL improved neurogenesis in a dose-dependent manner ($p < 0.05$–0.01, Fig. 6 [D1-E2, F]). Also, the extent of overall neurogenesis in these rats was closer to levels seen in naïve control animals ($p > 0.05$, Fig. 6 [F]). Thus, higher doses of MSL treatment for prolonged periods (8 weeks) is efficacious for improving hippocampal neurogenesis in GWI rats.

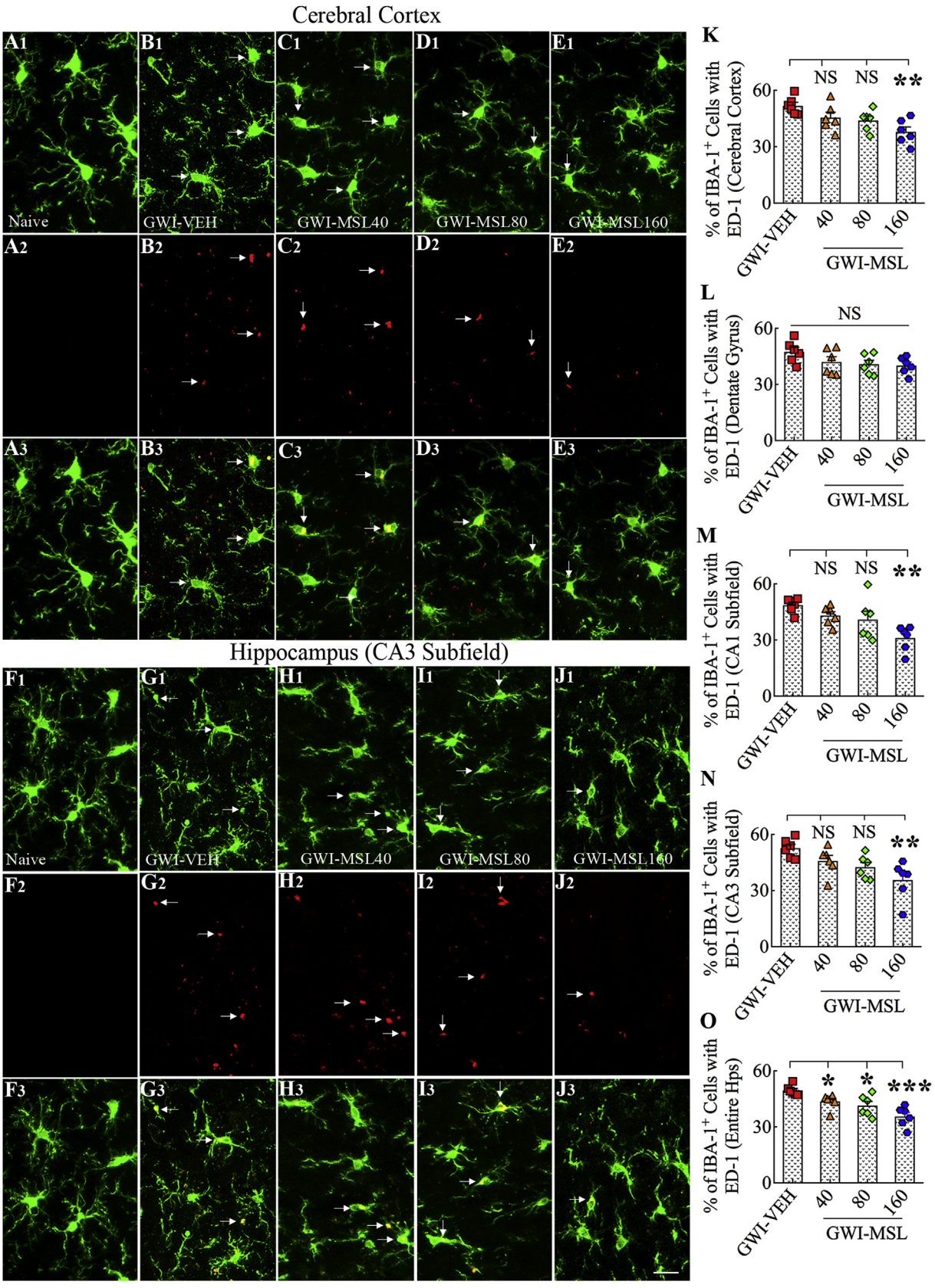

(caption on next page)

Fig. 5. Monosodium Luminal (MSL) treatment to rats with Gulf War Illness (i.e., GWI rats) reduced the occurrence of activated microglia expressing both IBA-1 and ED-1. Figures A1-E3 illustrate the distribution of IBA-1 + microglia expressing ED-1 in the cerebral cortex of animals belonging to the naïve control group (A1-A3), the GWI group receiving vehicle (GWI-VEH, B1–B3), and GWI groups receiving different doses of MSL (GWI-MSL40, C1–C3; GWI-MSL80, D1-D3; GWI-MSL160; E1-E3). Figures F1-J3 illustrate the distribution of IBA-1 + microglia expressing ED-1 in the hippocampal CA3 subfield of animals belonging to naïve control (F1–F3), GWI-VEH (G1-G3), and GWI-MSL groups (GWI-MSL40, H1–H3; GWI-MSL80, I1–I3; GWI-MSL160; J1-J3). The bar charts in K–O compare percentages of IBA1 + microglia expressing ED-1 in the cerebral cortex, the dentate gyrus, CA1, and CA3 subfields of the hippocampus and the entire hippocampus. Note that GWI rats receiving 160 mg/kg MSL exhibited a reduced percentage of activated microglia in the cerebral cortex and CA1 and CA3 subfields of the hippocampus. *, $p < 0.05$, **, $p < 0.01$, and ***, $p < 0.001$; NS, not significant. Scale bar, A1-J3 = 25 μm.

3.12. Eight weeks of MSL treatment also normalized neural stem cell activity in GWI rats

To ascertain whether the improved hippocampal neurogenesis observed with MSL treatment in GWI rats is linked to enhanced neural stem cell (NSC) activity, we quantified NSC activity in the SGZ-GCL through immunostaining for Ki67 (a marker of proliferating cells in all phases of the cell cycle) and stereological quantification of Ki67 + cells. ANOVA analysis showed significant differences between groups ($F = 28.1$, $p < 0.0001$). In comparison to naïve control animals, GWI rats receiving vehicle displayed reduced proliferation of NSCs ($p < 0.0001$, Fig. 7 [A-B, F]). Treatment of GWI rats at 40 mg/kg MSL did not improve NSC proliferation ($p > 0.05$ versus GWI rats receiving vehicle and $p < 0.0001$ versus naïve control animals, Fig. 7 [A-C, F]). Treatment of GWI rats at 80 mg/kg MSL, though resulted in higher NSC activity than GWI rats receiving vehicle ($p < 0.01$), did not improve NSC activity to naïve control levels ($p < 0.001$, Fig. 7 [A, B, D, F]). However, treatment of GWI rats at 160 mg/kg MSL improved

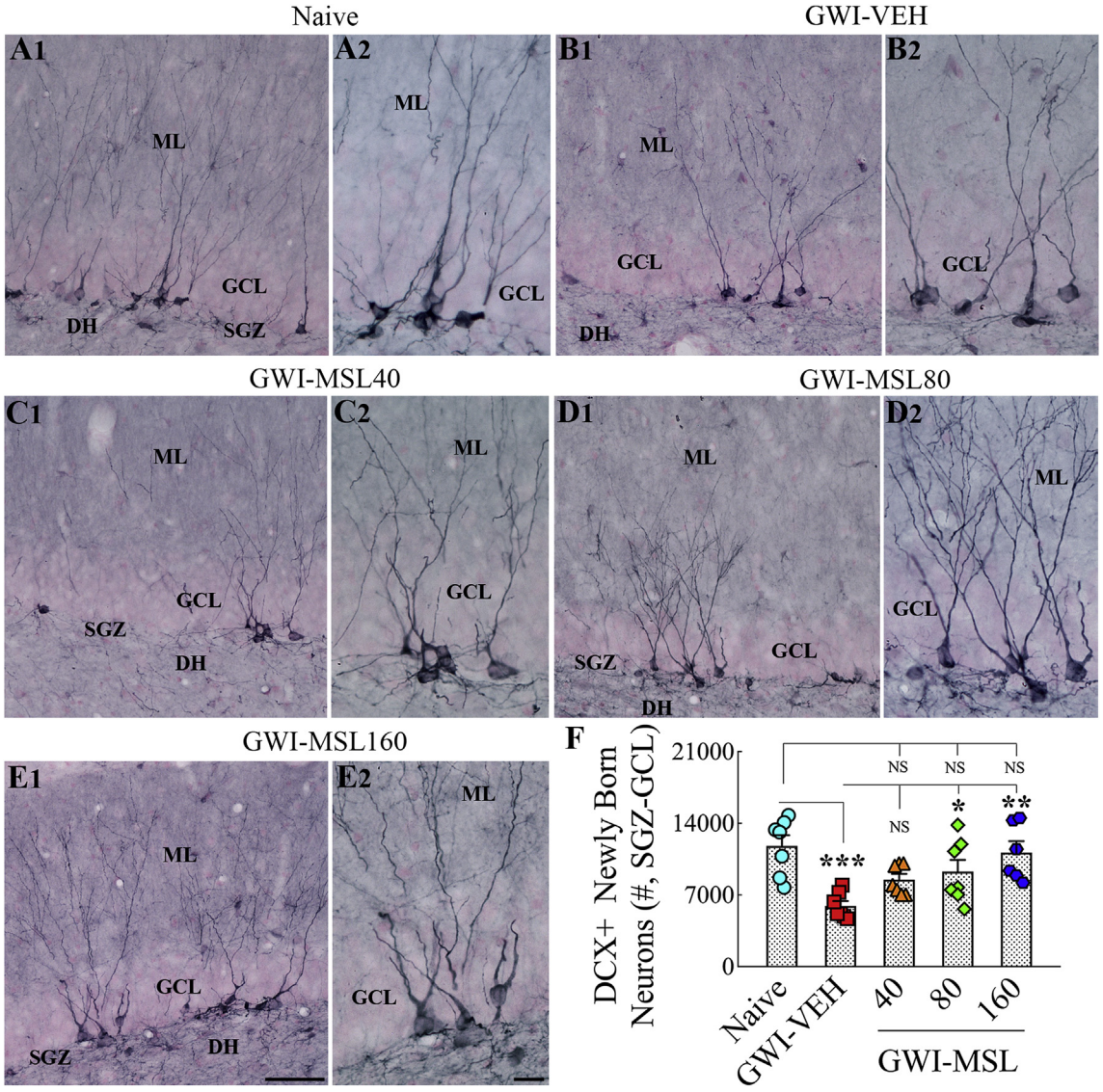

Fig. 6. Eight weeks of Monosodium Luminal (MSL) treatment to rats with Gulf War Illness (i.e., GWI rats) improved hippocampal neurogenesis. Figures A1- E2 illustrate the distribution of doublecortin-positive (DCX+) newly born neurons from animals belonging to the naïve control group (A1, A2), the GWI group receiving vehicle (GWI-VEH; B1, B2), and GWI groups receiving different doses of MSL (GWI-MSL40, C1–C2; GWI-MSL80, D1-D2; GWI-MSL160; E1-E2). A2, B2, C2, D2, and E2 are magnified views of regions from A1, B1, C1, D1, and E1. The bar chart F compares the number of DCX + neurons across different groups. Note that, GWI rats receiving 80 or 160 mg/kg MSL exhibited improved hippocampal neurogenesis. *, $p < 0.05$, **, $p < 0.01$, and ***, $p < 0.001$. Scale bar, A1, B1, C1, D1 and E1 = 50 μm; A2, B2, C2, D2 and E2 = 25 μm.

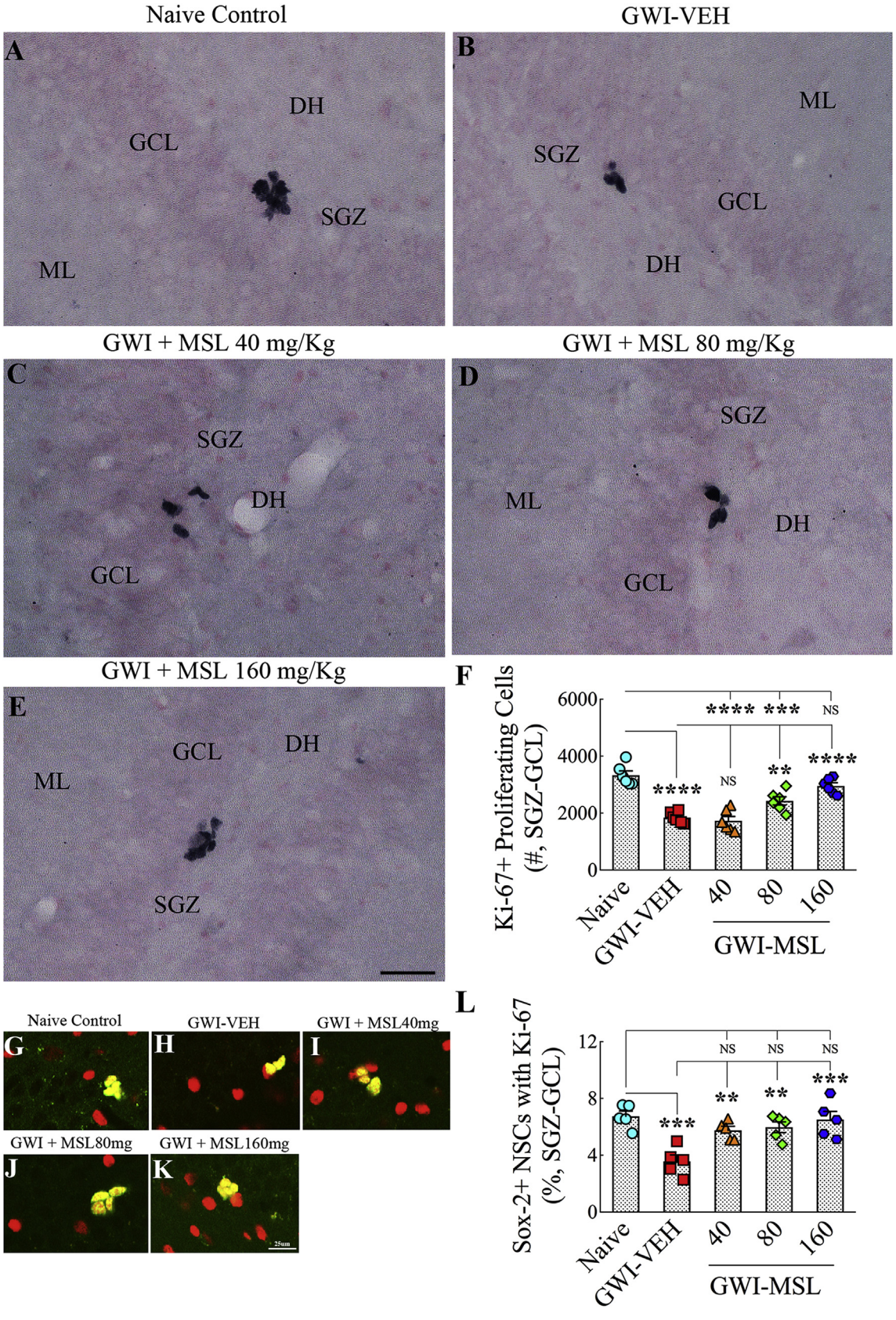

(caption on next page)

NSC activity to naïve control levels ($p < 0.0001$ versus GWI rats receiving vehicle and $p > 0.05$ versus naïve control animals, Fig. 7 [A-B, E-F). To obtain further insights, we quantified the percentages of putative NSCs in the SGZ (i.e., cells expressing the transcription factor Sox-2) expressing Ki-67 (Fig. 7 [G-K]). ANOVA analysis revealed significant differences between groups ($F = 8.9$, $p < 0.001$). We found a

Fig. 7. Eight weeks of Monosodium Luminal (MSL) treatment to rats with Gulf War Illness (i.e., GWI rats) improved the proliferation of putative neural stem cells (NSCs). Figures in A-E illustrate Ki67 + cell clusters (i.e. proliferating NSCs) in the subgranular zone-granule cell layer (SGZ-GCL) of the hippocampus from animals belonging to the naïve control group (A), the GWI group receiving vehicle (GWI-VEH; B), and GWI groups receiving different doses of MSL (GWI-MSL40, C; GWI-MSL80, D; GWI-MSL160; E). The bar chart in F compares the number of Ki67 + cells across different groups. Note that, GWI rats receiving 160 mg/kg MSL exhibited improved proliferation of NSCs. Figures in G-K illustrate examples of Sox-2+ putative NSCs expressing Ki-67 in different groups. The bar chart in L compares percentages of Sox-2+ cells expressing Ki-67 (i.e., proliferating NSCs) in the SGZ-GCL of the hippocampus between different groups of rats. A significant reduction in the proliferation of NSCs is seen in GWI rats receiving VEH, in comparison to naive control rats. However, MSL treatment at all doses improved the proliferative activity of NSCs. **, $p < 0.01$; ***, $p < 0.001$; and ****, $p < 0.0001$; NS, not significant. GCL, granule cell layer; ML, molecular layer; SGZ, subgranular zone. Scale bar, A-E = 50 μm; G-K = 25 μm.

significantly reduced NSC activity in GWI rats receiving the vehicle in comparison to naïve control animals ($p < 0.001$, Fig. 7 [L]). However, GWI rats receiving MSL at different doses displayed improved activity of NSCs ($p < 0.01$–0.001 versus GWI rats receiving vehicle and $p > 0.05$ versus naïve control animals, Fig. 7 [L]). The overall NSC activity appeared higher in GWI rats receiving 160 mg/kg MSL, however. Thus, enhanced NSC activity underlies normalized hippocampal neurogenesis in GWI rats after a higher dose administration of MSL for prolonged periods.

3.13. Eight weeks of MSL treatment alleviated systemic inflammation in GWI rats

Since the serum from GWI rats receiving a higher dose of MSL showed reduced MDA concentration than GWI rats receiving the vehicle, we investigated whether such high dose MSL treatment also modulated systemic inflammation in GWI rats. We used a rapid and sensitive rat cytokine array, which facilitated analyses of 16 rat cytokines in a high-throughput way. Serum samples from animals belonging to age-matched naïve control rats, GWI-rats receiving vehicle, or MSL at 160 mg/kg for eight weeks were compared (n = 6/group). ANOVA analysis revealed that many proinflammatory cytokines and chemokines were elevated in the serum from GWI-rats receiving vehicle ($F = 5.3$–195.0, $p < 0.05$–0.0001, Fig. 8), implying chronic systemic inflammation in GWI rats, as reported earlier [29]. The upregulated cytokines and chemokines include interleukin-1 alpha (IL-1α), IL-1 beta (IL-1β), tumor necrosis factor-alpha (TNF-α), macrophage chemoattractant protein 1 (MCP-1), macrophage inflammatory protein 1 alpha (MIP-1α or CCL3), transforming growth factor-beta (TGF-β), vascular endothelial growth factor (VEGF, and fibroblast growth factor-beta (FGF-β) ($p < 0.05$–0.0001, Fig. 8 [A-H]). Remarkably, administration of MSL at 160 mg/kg to GWI rats for eight weeks normalized the concentration of all of these proinflammatory cytokines and chemokines except FGF-β ($p > 0.05$ versus naïve control animals and $p < 0.05$–0.0001 versus GWI rats receiving the vehicle, Fig. 8 [A-H]). Thus, a higher dose of MSL treatment for prolonged periods (8 weeks) also reduced systemic inflammation in GWI rats.

4. Discussion

The results demonstrated that eight weeks of MSL treatment, particularly at a dose of 160 mg/kg, was proficient for alleviating cognitive and mood dysfunction in an animal model of GWI. Better cognition was apparent from an improved ability to perceive minor changes in the environment as well as the competence for recalling similar but not identical experiences in a nonoverlapping manner. Moreover, MSL treated animals exhibited reduced depressive- and anxiety-like behavior. Remarkably, improved brain function was linked with the reinstatement of redox homeostasis in the brain and the circulating blood. Restoration of redox balance was apparent from the normalized expression of multiple genes that encode proteins involved in combating oxidative stress in the brain and the concentration of oxidative stress

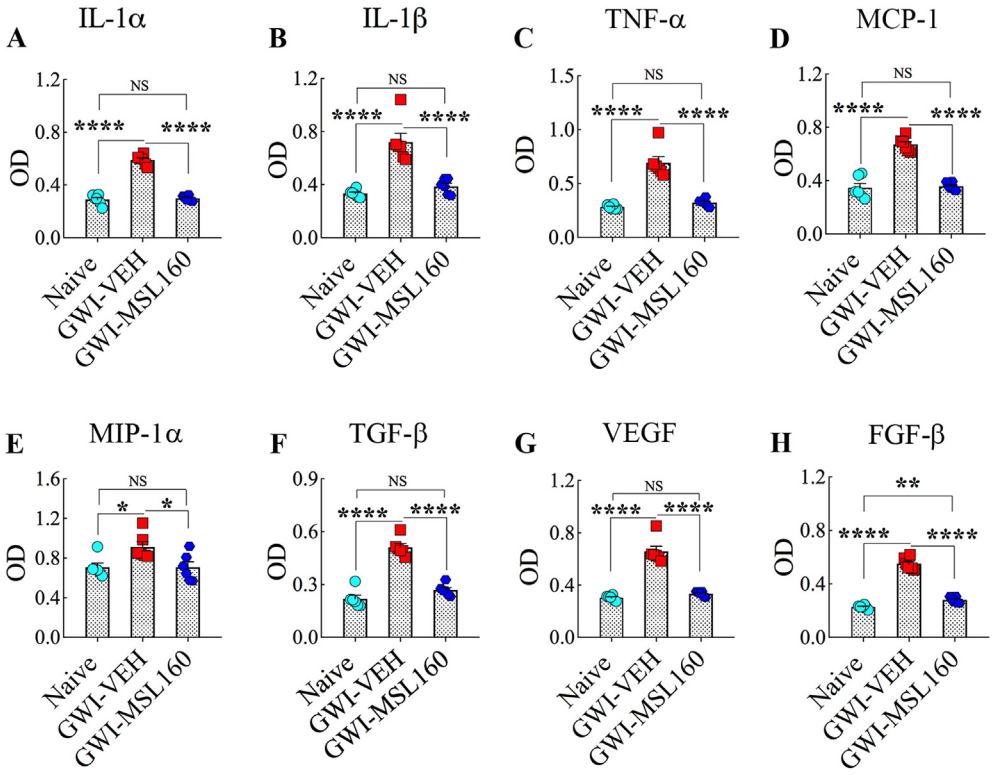

Fig. 8. Monosodium Luminal (MSL) treatment to rats with Gulf War Illness (i.e., GWI rats) normalized the levels of multiple cytokines and chemokines in the circulating blood. The bar charts in A-H respectively compare the concentration of interleukin-1 alpha (IL-1α), IL-1 beta (IL-1β), tumor necrosis factor-alpha (TNF-α), macrophage chemoattractant protein 1 (MCP-1), macrophage inflammatory protein 1 alpha (MIP-1α or CCL3), transforming growth factor-beta (TGF-β), vascular endothelial growth factor (VEGF, and fibroblast growth factor-beta (FGF-β). Note that all of these cytokines and chemokines are upregulated in GWI rats receiving the vehicle, and the administration of MSL at 160 mg/kg normalized their concentration in the circulating blood.

markers returning to naïve control levels in both brain and blood. Reestablishment of redox homeostasis has considerable implications. While the physiological concentrations ROS regulates several cell signaling pathways, chronically elevated ROS levels are injurious because they oxidize proteins and lipids, damage DNA, and activate astrocytes and microglia [55]. Indeed, the restoration of redox homeostasis in the brain by MSL also induced several other beneficial effects in GWI rats. These include the reduced density of hypertrophied astrocytes and activated microglia and increased proliferation of NSCs, leading to improved hippocampal neurogenesis. Besides, MSL treatment normalized the concentration of multiple proinflammatory cytokines and chemokines in the circulating blood.

Persistent cognitive and mood impairments are one of the salient features seen in veterans stricken with GWI [3,4,56]. A recent study has also reported impaired functional connectivity between different networks in the sensorimotor domain [57]. Investigations in animal prototypes of GWI have also reported continual cognitive and memory dysfunction and depressive- and anxiety-like behavior [16–20,28]. The pathological changes that parallel cognitive and mood abnormalities in the animal model of GWI employed in this study comprise increased oxidative stress, astrocyte hypertrophy, increased density of activated microglia, reduced proliferation of NSCs with waned neurogenesis, and chronic systemic inflammation [17,29]. Furthermore, at extended periods after the commencement of illness, the brain also displayed an increased concentration of proinflammatory cytokines, elevated HMGB1 exhibiting leakage into the extracellular space, as well as complement activation [18]. Thus, brain dysfunction in chronic GWI appears to be a cumulative effect of the detrimental microenvironment induced by elevated levels of ROS and proinflammatory molecules in the brain and/or the circulating blood. Nonetheless, it is unknown whether the state of redox imbalance befalls before the manifestation of chronic inflammation or an unrelenting inflammation continually maintains elevated levels of ROS. We chose to focus on redox imbalance as the underlying cause of brain dysfunction and chronic inflammation in GWI because GWI-related chemicals can trigger chronic oxidative stress in cells [32], and chronically elevated ROS levels can induce HMGB1 leakage, unrelenting inflammation and brain dysfunction [34,58]. Considering these, we chose MSL, a drug that has shown promise for re-establishing redox homeostasis in several disease models earlier [35–40].

Indeed, a higher dose of MSL reinstated redox balance in this study, which was evident from several observations. MSL treatment normalized the expression of 20 genes that typically display upregulation in conditions of elevated oxidative stress, as observed in GWI rats receiving the vehicle in this study. The notable proteins encoded by these genes are involved in redox regulation (*Prdx6, Srxn1, Txn1*), mediating oxidative stress (*Txnip*), clearing mitochondrial ROS (*Sod2*), cellular detoxification (*Gstp1*), protection against ROS (*Idh1, Prdx6, Sod2, Txnrd1, Txnrd2*), antioxidant effects (*Gsr, Prdx1, 2, and 4*), carrying mitochondrial protons (*Ucp2*), regulating the activation of NF-kB pathway (*Sqstm1*), formation of protein aggregates (*Sqstm1, Prnp*), proteolytic processing of amyloid precursor protein (*Ctsb*), cholesterol biosynthesis (*Dhcr24*) and prostaglandin biosynthesis (*Ptgs2*). To obtain further insights on the reinstatement of redox homeostasis by MSL, we quantified oxidative stress markers MDA, 4-HNE, and PCs. MDA and 4-HNE, being the byproducts of lipid peroxidation, can suggest the status of oxidative stress through changes in their levels [59,60]. PCs, on the other hand, represent an irreversible form of protein modification that is relatively stable. PCs also serve as a marker of global protein oxidation as they are generated by multiple different ROS [61]. Consistent with the gene expression results, MSL treatment at 160 mg/kg normalized the concentration of all three oxidative stress markers in the brain. The same dose was also effective for normalizing the concentration of both MDA and PCs in the circulating blood.

Furthermore, we investigated whether changes mediated by MSL affected the innate response of the organism to combat oxidative stress by measuring SOD2 and NRF2. SOD2 is a mitochondrial antioxidant that is typically upregulated in conditions of increased oxidative stress. NRF-2, a transcription factor considered a master regulator of oxidative stress, generates antioxidant and phase II detoxification enzymes under conditions of augmented oxidative stress, which help in decreasing oxidative stress, the buildup of toxic metabolites and modulation of activated microglia [62–65]. NRF-2 activation has been seen in neurodegenerative disorders such as Parkinson's disease [66] and amyotrophic lateral sclerosis [67]. Both SOD-2 and NRF-2 were found to be upregulated in the brain of GWI rats, but MSL treatment did not modify their levels, implying that MSL treatment reinstates redox homeostasis without interfering with the brain's innate defense mechanisms against increased oxidative stress. These observations are consistent with suggestions in previous studies that MSL mediates redox homeostasis by acting as a redox buffer, which keeps the oxidation-reduction reactions in balance [35–40].

Re-establishment of redox homeostasis by MSL in the brain normalized the population of reactive astrocytes and transformed a significant percentage of microglia from their activated phenotype to resting state. The occurrence of large numbers of reactive astrocytes and activated microglia imply neuroinflammation. Animal prototypes of GWI have consistently shown neuroinflammation [16–18,21,23,68,69]. Studies have also suggested the presence of neuroinflammation in veterans with GWI [70–72]. Neuroinflammation, depending on the severity, can directly impair cognitive and mood function or indirectly affect cognition and mood by interfering with hippocampal neurogenesis [73–75]. Remarkably, reinstatement of redox homeostasis and improved cognitive and mood function by a higher dose of MSL paralleled a reduced density of reactive astrocytes and activated microglia in the brain. Suppression of inflammation has also been observed in other disease models following MSL treatment [35,39]. Nonetheless, the suppression of neuroinflammation following MSL treatment is likely an indirect effect of inducing redox homeostasis. This concept is supported by earlier observations that persistently elevated ROS levels produce damage-associated molecular patterns and induce activation of astrocytes and microglia [76]. While the organism's inflammatory response is considered a defense mechanism in a state of redox balance, dysregulation of the immune response occurs with a chronic loss of redox balance [55]. Regardless of the underlying mechanisms, reduced densities of reactive astrocytes and activated microglia have likely also played a role in improving cognitive and mood function in GWI rats receiving MSL.

Redox homeostasis promoted by MSL also enhanced the proliferation of NSCs leading to increased hippocampal neurogenesis. Numerous studies have demonstrated that adult hippocampal neurogenesis occurs throughout life in rodents as well as humans [77–81], which plays a critical role in making certain types of new memories, maintenance of mood function, and pattern separation ability [82–84]. Earlier studies in a rat model of GWI have also suggested a link between persistent cognitive and mood dysfunction and waned hippocampal neurogenesis [16,17]. Moreover, the current study demonstrated impaired pattern separation function in GWI rats, which paralleled decreased neurogenesis in the hippocampus. Pattern separation helps in successfully recalling overlapping experiences, which is an ability to distinguish similar experiences through the storage of representations in a non-overlapping manner [53]. Remarkably, eight weeks of treatment at 160 mg/kg upregulated neurogenesis to naïve control levels through increased proliferation of NSCs. Also, enhanced neurogenesis in MSL treated animals paralleled the redox homeostasis mediated by a higher dose of MSL. Because the extent of neurogenesis is highly sensitive to ROS levels in the environment [85], increased neurogenesis is likely a result of an improved milieu in NSC niches due to the reinstatement of redox balance and the subsequent suppression of neuroinflammation mediated by eight weeks of MSL treatment. No changes in neurogenesis observed with only three weeks of MSL treatment also supports this notion. Thus, improved hippocampal neurogenesis is likely one of the

underlying factors that improved cognitive and mood dysfunction in GWI rats following eight weeks of MSL treatment.

Another beneficial effect of MSL-mediated redox homeostasis in this study was the alleviation of systemic inflammation. Eight weeks of MSL treatment at 160 mg/kg to GWI rats normalized the levels of many proinflammatory cytokines and chemokines in the circulating blood, which include IL-1α, IL-1β, TNF-α, MCP-1, MIP-1α (Ccl3), TGF-β, VEGF, and FGF-β. Systemic inflammation is another consistent feature of chronic GWI [86–88]. Blood sample analyses from GWI patients have consistently revealed the presence of systemic inflammation. The findings include increased levels of IL-1β and IL-15 on higher fatigue severity days [89], and enhanced concentration of soluble receptor II for TNF [70]. Besides, higher numbers of lymphocytes, monocytes, neutrophils, and platelets, and elevated levels of C-reactive protein, leptin, brain-derived neurotrophic factor, and matrix metalloproteinase-9 have been observed [71]. These findings supported the suggestion that persistent systemic inflammation is another factor contributing to brain dysfunction in GWI, as several studies have revealed that significant systemic inflammation leads to enduring cognitive dysfunction [90–93]. Both hematogenous and neural pathways are likely involved in the interaction between systemic inflammation and the brain [94]. The brain-immune system interaction likely involves the transfer of proteins, microRNAs, and lipids between brain cells and immune cells through extracellular vesicles shed by them [18,95,96]. From these perspectives, alleviation of systemic inflammation found in MSL treated GWI rats is significant, which is likely the result of the reinstatement of redox homeostasis at the systemic level by MSL. Thus, amelioration of systemic inflammation is likely another factor that contributed to improved cognitive and mood function in this study.

4.1. Conclusions and future directions

Eight weeks of MSL treatment in GWI rats considerably improved cognitive and mood function in this study, which paralleled the reinstatement of redox homeostasis in the brain and the circulating blood. Furthermore, the reestablishment of redox balance by MSL modulated reactive astrocytes, activated microglia, and NSCs with a net effect of reduced neuroinflammation and enhanced hippocampal neurogenesis in the brain and significantly suppressed systemic inflammation. These beneficial effects found in an animal model of GWI support testing the efficacy of MSL for improving brain function in veterans with GWI. A double-blind, placebo-controlled, clinical trial with different doses will be required to ascertain the usefulness of MSL to improve health in veterans with GWI. Furthermore, because MSL acts as a buffer to maintain redox homeostasis, it will be essential to discern whether MSL treatment for a specified period (e.g., 4–12 months) is sufficient for inducing lasting improvements in brain function, or continuous MSL treatment will be required to maintain better brain function in veterans with GWI.

Author contributions

Concept: AKS. Research design: AKS, SA, MK, BS, GS, and BH. Data collection: SA, MK, BS, GS, DU, BH, MLN, RU, AB, and XR. Data analysis and interpretation: AKS, SA, MK, BS, GS, DU, BH, MLN, and RU. Preparation of figure composites: AKS, SA, and MK. Manuscript writing: AKS. All authors provided feedback and edits to the manuscript text and approved the final version of the manuscript.

Declaration of competing interest

The authors declared no conflicts of interest.

Acknowledgments

This work was supported by grants from the Department of Defense (GWIRP grants, (W81XWH-14-1-0572 and W81XWH-16-1-0480 to A.K.S). Authors thank Bach Pharma, Inc (North Andover, MA 01845) for supplying MSL-GVT for no cost for these studies. Authors also thank Dr. Paul Wong, Retired Professor, MD Anderson Cancer Center, Smithville TX, for useful suggestions on MSL handling and dosing in animal models of disease.

Appendix A. Supplementary data

Supplementary data to this article can be found online at https://doi.org/10.1016/j.redox.2019.101389.

References

[1] R.F. White, L. Steele, J.P. O'Callaghan, K. Sullivan, J.H. Binns, B.A. Golomb, et al., Recent research on Gulf War illness and other health problems in veterans of the 1991 Gulf War: effects of toxicant exposures during deployment, Cortex 74 (2016) 449–475.
[2] L. Steele, Prevalence and patterns of Gulf War illness in Kansas veterans: association of symptoms with characteristics of person, place, and time of military service, Am. J. Epidemiol. 152 (2000) 992–1002.
[3] T.N. Odegard, C.M. Cooper, E.A. Farris, J. Arduengo, J. Bartlett, R. Haley, Memory impairment exhibited by veterans with gulf war illness, Neurocase 19 (2013) 316–327.
[4] P.A. Janulewicz, M.H. Krengel, A. Maule, R.F. White, J. Cirillo, E. Sisson, et al., Neuropsychological characteristics of Gulf War illness: a meta-analysis, PLoS One 12 (2017) e0177121.
[5] X. Li, J.S. Spence, D.M. Buhner, J. Hart Jr., C.M. Cullum, M.M. Biggs, et al., Hippocampal dysfunction in Gulf War veterans: investigation with ASL perfusion MR imaging and physostigmine challenge, Radiology 261 (2011) 218–225.
[6] R.U. Rayhan, M.K. Ravindran, J.N. Baraniuk, Migraine in gulf war illness and chronic fatigue syndrome: prevalence, potential mechanisms, and evaluation, Front. Physiol. 4 (2013) 181.
[7] N.A. Hubbard, J.L. Hutchison, M.A. Motes, E. Shokri-Kojori, I.J. Bennett, R.M. Brigante, et al., Central executive dysfunction and deferred prefrontal processing in veterans with gulf war illness, Clin Psychol Sci 2 (2014) 319–327.
[8] S.M. VanRiper, A.L. Alexander, K.F. Koltyn, A.J. Stegner, L.D. Ellingson, D.J. Destiche, et al., Cerebral white matter structure is disrupted in Gulf War Veterans with chronic musculoskeletal pain, Pain 158 (2017) 2364–2375.
[9] L. Steele, A. Sastre, M.M. Gerkovich, M.R. Cook, Complex factors in the etiology of Gulf War illness: wartime exposures and risk factors in veteran subgroups, Environ. Health Perspect. 120 (2012) 112–118.
[10] J.H. Binns, C. Barlow, F.E. Bloom, D.J. Clauw, B.A. Golomb, J.C. Graves, et al., Gulf War Illness and the Health of Gulf War Veterans: Scientific Findings and Recommendations, Research Advisory Committee Report on Gulf War Illness and Health of Gulf War Veterans, Dept of Veterans Affairs. US Government Printing Office, Washington, DC, 2008 pp. 1–465.
[11] W.R. Schumm, E.J. Reppert, A.P. Jurich, S.R. Bollman, F.J. Webb, C.S. Castelo, et al., Pyridostigmine bromide and the long-term subjective health status of a sample of over 700 male Reserve Component Gulf War era veterans, Psychol. Rep. 90 (2002) 707–721.
[12] K. Sullivan, M. Krengel, P.S. Proctor, S. Devine, T. Heeren, R.F. White, Cognitive functioning in treatment-seeking gulf war veterans: pyridostigmine bromide use and PTSD, J. Psychopathol. Behav. Assess. 25 (2003) 95–103.
[13] B.A. Golomb, Acetylcholinesterase inhibitors and gulf war illnesses, Proc. Natl. Acad. Sci. U. S. A. 105 (2008) 4295–4300.
[14] A. Abdel-Rahman, A.K. Shetty, M.B. Abou-Donia, Disruption of the blood-brain barrier and neuronal cell death in cingulate cortex, dentate gyrus, thalamus, and hypothalamus in a rat model of Gulf-War syndrome, Neurobiol. Dis. 10 (2002) 306–326.
[15] A. Abdel-Rahman, S. Abou-Donia, E. El-Masry, A.K. Shetty, et al., Stress and combined exposure to low doses of pyridostigmine bromide, DEET, and permethrin produce neurochemical and neuropathological alterations in cerebral cortex, hippocampus, and cerebellum, J. Toxicol. Environ. Health 67 (2004) 163–192.
[16] V.K. Parihar, B. Hattiangady, B. Shuai, A.K. Shetty, Mood and memory deficits in a model of Gulf War illness are linked with reduced neurogenesis, partial neuron loss, and mild inflammation in the hippocampus, Neuropsychopharmacology 38 (2013) 2348–2362.
[17] M. Kodali, B. Hattiangady, G.A. Shetty, A. Bates, B. Shuai, A.K. Shetty, Curcumin treatment leads to better cognitive and mood function in a model of Gulf War Illness with enhanced neurogenesis, and alleviation of inflammation and mitochondrial dysfunction in the hippocampus, Brain Behav. Immun. 69 (2018) 499–514.
[18] L.N. Madhu, S. Attaluri, M. Kodali, B. Shuai, R. Upadhya, D. Gitai, et al., Neuroinflammation in Gulf War Illness is linked with HMGB1 and complement activation, which can be discerned from brain-derived extracellular vesicles in the blood, Brain Behav. Immun. 81 (2019) 430–443.
[19] L. Abdullah, G. Crynen, J. Reed, A. Bishop, J. Phillips, S. Ferguson, et al., Proteomic CNS profile of delayed cognitive impairment in mice exposed to Gulf War agents, NeuroMolecular Med. 13 (2011) 275–288.
[20] Z. Zakirova, G. Crynen, S. Hassan, L. Abdullah, L. Horne, V. Mathura, et al., A chronic longitudinal characterization of neurobehavioral and neuropathological

cognitive impairment in a mouse model of gulf war agent exposure, Front. Integr. Neurosci. 9 (2015) 71.
[21] J.P. O'Callaghan, K.A. Kelly, A.R. Locker, D.B. Miller, S.M. Lasley, Corticosterone primes the neuroinflammatory response to DFP in mice: potential animal model of Gulf War Illness, J. Neurochem. 133 (2015) 708–721.
[22] K.F. Phillips, L.S. Deshpande, Repeated low-dose organophosphate DFP exposure leads to the development of depression and cognitive impairment in a rat model of Gulf War Illness, Neurotoxicology 52 (2016) 127–133.
[23] A.R. Locker, L.T. Michalovicz, K.A. Kelly, J.V. Miller, D.B. Miller, J.P. O'Callaghan, Corticosterone primes the neuroinflammatory response to Gulf War Illness-relevant organophosphates independently of acetylcholinesterase inhibition, J. Neurochem. 142 (2017) 444–455.
[24] D.W. Black, C.P. Carney, V.L. Forman-Hoffman, E. Letuchy, P. Peloso, R.F. Woolson, et al., Depression in veterans of the first Gulf War and comparable military controls, Ann. Clin. Psychiatr. 16 (2004) 53–61.
[25] P.M. Menon, H.A. Nasrallah, R.R. Reeves, J.A. Ali, Hippocampal dysfunction in Gulf War Syndrome. A proton MR spectroscopy study, Brain Res. 1009 (2004) 189–194.
[26] K.E. Thompson, J.J. Vasterling, E.G. Benotsch, K. Brailey, J. Constans, M. Uddo, et al., Early symptom predictors of chronic distress in Gulf War veterans, J. Nerv. Ment. Dis. 192 (2004) 146–152.
[27] K. Sullivan, M. Krengel, W. Bradford, C. Stone, T.A. Thompson, T. Heeren, et al., Neuropsychological functioning in military pesticide applicators from the Gulf War: effects on information processing speed, attention and visual memory, Neurotoxicol. Teratol. 65 (2018) 1–13.
[28] B. Hattiangady, V. Mishra, M. Kodali, B. Shuai, X. Rao, A.K. Shetty, Object location and object recognition memory impairments, motivation deficits and depression in a model of Gulf War illness, Front. Behav. Neurosci. 8 (2014) 78.
[29] G.A. Shetty, B. Hattiangady, D. Upadhya, A. Bates, S. Attaluri, B. Shuai, et al., Chronic oxidative stress, mitochondrial dysfunction, Nrf2 activation and inflammation in the Hippocampus accompany heightened systemic inflammation and oxidative stress in an animal model of gulf war illness, Front. Mol. Neurosci. 10 (2017) 182.
[30] R.A. Kohman, J.S. Rhodes, Neurogenesis, inflammation and behavior, Brain Behav. Immun. 27 (2013) 22–32.
[31] K.A. Jenrow, S.L. Brown, K. Lapanowski, H. Naei, A. Kolozsvary, J.H. Kim, Selective inhibition of microglia-mediated neuroinflammation mitigates radiation-induced cognitive impairment, Radiat. Res. 179 (2013) 549–556.
[32] K. Soltaninejad, M. Abdollahi, Current opinion on the science of organophosphate pesticides and toxic stress: a systematic review, Med. Sci. Monit. 15 (2009) 75–90.
[33] A. Popa-Wagner, S. Mitran, S. Sivanesan, E. Chang, A.M. Buga, ROS and brain diseases: the good, the bad, and the ugly, Oxid Med Cell Longev 2013 (2013) 963520.
[34] L. Zuo, E.R. Prather, M. Stetskiv, D.E. Garrison, J.R. Meade, T.I. Peace, et al., Inflammaging and oxidative stress in human diseases: from molecular mechanisms to novel treatments, Int. J. Mol. Sci. 20 (2019) E4472.
[35] Y. Jiang, V.L. Scofield, M. Yan, W. Qiang, N. Liu, A.J. Reid, et al., Retrovirus-induced oxidative stress with neuroimmunodegeneration is suppressed by antioxidant treatment with a refined monosodium alpha-luminol (Galavit), J. Virol. 80 (2006) 4557–4569.
[36] G. Lungu, X. Kuang, G. Stoica, P.K. Wong, Monosodium luminol upregulates the expression of Bcl-2 and VEGF in retrovirus-infected mice through downregulation of corresponding miRNAs, Acta Virol. 54 (2010) 27–32.
[37] P.V. Reddy, G. Lungu, X. Kuang, G. Stoica, P.K. Wong, Neuroprotective effects of the drug GVT (monosodium luminol) are mediated by the stabilization of Nrf2 in astrocytes, Neurochem. Int. 56 (2010) 780–788.
[38] X. Kuang, M. Yan, J.M. Ajmo, V.L. Scofield, G. Stoica, P.K. Wong, Activation of AMP-activated protein kinase in cerebella of Atm-/- mice is attributable to accumulation of reactive oxygen species, Biochem. Biophys. Res. Commun. 418 (2012) 267–272.
[39] V.L. Scofield, M. Yan, X. Kuang, S.J. Kim, P.K. Wong, The drug monosodium luminol (GVT) preserves crypt-villus epithelial organization and allows survival of intestinal T cells in mice infected with the ts1 retrovirus, Immunol. Lett. 122 (2009) 150–158.
[40] J. Kim, P.K. Wong, Targeting p38 mitogen-activated protein kinase signaling restores subventricular zone neural stem cells and corrects neuromotor deficits in Atm knockout mouse, Stem Cells Transl. Med. 1 (2012) 548–556.
[41] T. Tanielian, L.H. Jaycox, D.M. Adamson, M.A. Burnam, R.M. Burns, L.B. Caldarone, et al., Invisible Wounds of War, (2008) [Internet].
[42] Q. Long, D. Upadhya, B. Hattiangady, D.K. Kim, S.Y. An, B. Shuai, et al., Intranasal MSC-derived A1-exosomes ease inflammation, and prevent abnormal neurogenesis and memory dysfunction after status epilepticus, Proc. Natl. Acad. Sci. U. S. A. 114 (2017) E3536–E3545.
[43] D. Upadhya, B. Hattiangady, O.W. Castro, B. Shuai, M. Kodali, S. Attaluri, et al., Human induced pluripotent stem cell-derived MGE cell grafting after status epilepticus attenuates chronic epilepsy and comorbidities via synaptic integration, Proc. Natl. Acad. Sci. U. S. A. 116 (2019) 287–296.
[44] M.S. Rao, Hattiangady, A.K. Shetty, Status epilepticus during old age is not associated with enhanced hippocampal neurogenesis, Hippocampus 18 (2008) 931–944.
[45] B. Hattiangady, R. Kuruba, A.K. Shetty, Acute seizures in old age leads to a greater loss of CA1 pyramidal neurons, an increased propensity for developing chronic TLE and a severe cognitive dysfunction, Aging Dis 2 (2011) 1–17.
[46] M. Kodali, V.K. Parihar, B. Hattiangady, V. Mishra, B. Shuai, A.K. Shetty, Resveratrol prevents age-related memory and mood dysfunction with increased hippocampal neurogenesis and microvasculature, and reduced glial activation, Sci. Rep. 5 (2015) 8075.
[47] G.A. Shetty, B. Hattiangady, A.K. Shetty, Neural stem cell- and neurogenesis-related gene expression profiles in the young and aged dentate gyrus, Age 35 (2013) 2165–2176.
[48] V. Mishra, B. Shuai, M. Kodali, G.A. Shetty, B. Hattiangady, X. Rao, et al., Resveratrol treatment after status epilepticus restrains neurodegeneration and abnormal neurogenesis with suppression of oxidative stress and inflammation, Sci. Rep. 5 (2015) 17807.
[49] A.K. Shetty, B. Hattiangady, M.S. Rao, B. Shuai, Neurogenesis response of middle-aged hippocampus to acute seizure activity, PLoS One 7 (2012) e43286.
[50] M. Kodali, T. Megahed, V. Mishra, B. Shuai, B. Hattiangady, A.K. Shetty, Voluntary running exercise-mediated enhanced neurogenesis does not obliterate retrograde spatial memory, J. Neurosci. 36 (2016) 8112–8122.
[51] M.S. Rao, B. Hattiangady, K.S. Rai, A.K. Shetty, Strategies for promoting anti-seizure effects of hippocampal fetal cells grafted into the hippocampus of rats exhibiting chronic temporal lobe epilepsy, Neurobiol. Dis. 27 (2007) 117–132.
[52] B. Hattiangady, B. Shuai, J. Cai, T. Coksaygan, M.S. Rao, A.K. Shetty, Increased dentate neurogenesis after grafting of glial restricted progenitors or neural stem cells in the aging hippocampus, Stem Cells 25 (2007) 2104–2117.
[53] M.A. Yassa, C.E. Stark, Pattern separation in the hippocampus, Trends Neurosci. 34 (2011) 515–525.
[54] Z. Merali, C. Levac, H. Anisman, Validation of a simple, ethologically relevant paradigm for assessing anxiety in mice, Biol. Psychiatry 54 (2003) 552–565.
[55] H. Solleiro-Villavicencio, S. Rivas-Arancibia, Effect of chronic oxidative stress on neuroinflammatory response mediated by CD4(+)T cells in neurodegenerative diseases, Front. Cell. Neurosci. 12 (2018) 114.
[56] B.E. Engdahl, L.M. James, R.D. Miller, A.C. Leuthold, S.M. Lewis, A.F. Carpenter, et al., Brain function in gulf war illness (GWI) and associated mental health comorbidities, J Neurol Neuromed. 3 (2018) 24–34.
[57] K.S. Gopinath, U. Sakoglu, B.A. Crosson, R.W. Haley, Exploring brain mechanisms underlying Gulf War Illness with group ICA based analysis of fMRI resting state networks, Neurosci. Lett. 701 (2019) 136–141.
[58] G. Terrone, S. Balosso, A. Pauletti, T. Ravizza, A. Vezzani, Inflammation and reactive oxygen species as disease modifiers in epilepsy, Neuropharmacology (2019) 107742. [Epub ahead of print].
[59] I. Dalle-Donne, R. Rossi, R. Colombo, D. Giustarini, A. Milzani, Biomarkers of oxidative damage in human disease, Clin. Chem. 52 (2006) 601–623.
[60] M. Breitzig, C. Bhimineni, R. Lockey, N. Kolliputi, 4-Hydroxy-2-nonenal: a critical target in oxidative stress? Am. J. Physiol. Cell Physiol. 311 (2016) C537–C543.
[61] D. Weber, M.J. Davies, T. Grune, Determination of protein carbonyls in plasma, cell extracts, tissue homogenates, isolated proteins: focus on sample preparation and derivatization conditions, Redox Biol. 5 (2015) 367–380.
[62] N.G. Innamorato, A.I. Rojo, A.J. Garcia-Yague, M. Yamamoto, M.L. de Ceballos, A. Cuadrado, The transcription factor Nrf2 is a therapeutic target against brain inflammation, J. Immunol. 181 (2008) 680–689.
[63] G. Joshi, J.A. Johnson, The Nrf2-ARE pathway: a valuable therapeutic target for the treatment of neurodegenerative diseases, Recent Pat. CNS Drug Discov. 7 (2012) 218–229.
[64] I. Lastres-Becker, N.G. Innamorato, T. Jaworski, A. Rabano, S. Kugler, F. Van Leuven, et al., Fractalkine activates NRF2/NFE2L2 and heme oxygenase 1 to restrain tauopathy-induced microgliosis, Brain 137 (2014) 78–91.
[65] I. Lastres-Becker, A. Ulusoy, N.G. Innamorato, G. Sahin, A. Rabano, D. Kirik, et al., alpha-Synuclein expression and Nrf2 deficiency cooperate to aggravate protein aggregation, neuronal death and inflammation in early-stage Parkinson's disease, Hum. Mol. Genet. 21 (2012) 3173–3192.
[66] A. Jazwa, A.I. Rojo, N.G. Innamorato, M. Hesse, J. Fernandez-Ruiz, A. Cuadrado, Pharmacological targeting of the transcription factor Nrf2 at the basal ganglia provides disease modifying therapy for experimental parkinsonism, Antioxidants Redox Signal. 14 (2011) 2347–2360.
[67] S. Petri, S. Korner, M. Kiaei, Nrf2/ARE signaling pathway: key mediator in oxidative stress and potential therapeutic target in ALS, Neurol Res. Int. (2012) 878030 2012.
[68] U. Joshi, A. Pearson, J.E. Evans, H. Langlois, N. Saltiel, J. Ojo, et al., A permethrin metabolite is associated with adaptive immune responses in Gulf War Illness, Brain Behav. Immun. (2019) S0889-1591: 30329-0, [Epub ahead of print].
[69] L.T. Michalovicz, A.R. Locker, K.A. Kelly, J.V. Miller, Z. Barnes, M.A. Fletcher, et al., Corticosterone and pyridostigmine/DEET exposure attenuate peripheral cytokine expression: supporting a dominant role for neuroinflammation in a mouse model of Gulf War Illness, Neurotoxicology 70 (2019) 26–32.
[70] A. O'Donovan, L.L. Chao, J. Paulson, K.W. Samuelson, J.K. Shigenaga, C. Grunfeld, et al., Altered inflammatory activity associated with reduced hippocampal volume and more severe posttraumatic stress symptoms in Gulf War veterans, Psychoneuroendocrinology 51 (2015) 557–566.
[71] G.J. Johnson, B.C. Slater, L.A. Leis, T.S. Rector, R.R. Bach, Blood biomarkers of chronic inflammation in gulf war illness, PLoS One 11 (2016) e0157855.
[72] M.B. Abou-Donia, L.A. Conboy, E. Kokkotou, E.M. El-Masry, E. Jacobson, K. Sullivan, Screening for novel central nervous system biomarkers in veterans with Gulf War Illness, Neurotoxicol. Teratol. 61 (2017) 36–46.
[73] B. Kaltschmidt, C. Kaltschmidt, NF-KappaB in long-term memory and structural plasticity in the adult mammalian brain, Front. Mol. Neurosci. 8 (2015) 69.
[74] K.M. McAvoy, A. Sahay, Targeting adult neurogenesis to optimize hippocampal circuits in aging, Neurotherapeutics 14 (2017) 630–645.
[75] L. Peng, M.A. Bonaguidi, Function and dysfunction of adult hippocampal neurogenesis in regeneration and disease, Am. J. Pathol. 188 (2018) 23–28.
[76] N. Bakunina, C.M. Pariante, P.A. Zunszai, Immune mechanisms linked to depression via oxidative stress and neuroprogression, Immunology 144 (2015) 365–373.
[77] B. Hattiangady, A.K. Shetty, Aging does not alter the number or phenotype of putative stem/progenitor cells in the neurogenic region of the hippocampus,

Neurobiol. Aging 29 (2008) 129–147.
[78] P.S. Eriksson, E. Perfilieva, T. Björk-Eriksson, A.M. Alborn, C. Nordborg, D.A. Peterson, et al., Neurogenesis in the adult human hippocampus, Nat. Med. 4 (1998) 1313–1317.
[79] M. Boldrini, C.A. Fulmore, A.N. Tartt, L.R. Simeon, I. Pavlova, V. Poposka, et al., Human hippocampal neurogenesis persists throughout aging, Cell Stem Cell 22 (2018) 589–599.
[80] E.P. Moreno-Jiménez, M. Flor-García, J. Terreros-Roncal, A. Rábano, F. Cafini, N. Pallas-Bazarra, et al., Adult hippocampal neurogenesis is abundant in neurologically healthy subjects and drops sharply in patients with Alzheimer's disease, Nat. Med. 25 (2019) 554–560.
[81] M.K. Tobin, K. Musaraca, A. Disouky, A. Shetti, A. Bheri, W.G. Honer, et al., Human hippocampal neurogenesis persists in aged adults and alzheimer's disease patients, Cell Stem Cell 24 (2019) 974–982.
[82] W. Deng, J.B. Aimone, F.H. Gage, New neurons and new memories: how does adult hippocampal neurogenesis affect learning and memory? Nat. Rev. Neurosci. 11 (2010) 339–350.
[83] M.A. Kheirbek, K.C. Klemenhagen, A. Sahay, R. Hen, Neurogenesis and generalization: a new approach to stratify and treat anxiety disorders, Nat. Neurosci. 15 (2012) 1613–1620.
[84] T.F.A. Franca, A.M. Bitencourt, N.R. Maximilla, D.M. Barros, J.M. Monserrat, Hippocampal neurogenesis and pattern separation: a meta-analysis of behavioral data, Hippocampus 27 (2017) 937–950.
[85] T.T. Huang, D. Leu, Y. Zou, Oxidative stress and redox regulation on hippocampal-dependent cognitive functions, Arch. Biochem. Biophys. 576 (2015) 2–7.
[86] A.L. Smylie, G. Broderick, H. Fernandes, S. Razdan, Z. Barnes, F. Collado, et al., A comparison of sex-specific immune signatures in Gulf War illness and chronic fatigue syndrome, BMC Immunol. 14 (2013) 29.
[87] G. Broderick, R. Ben-Hamo, S. Vashishtha, S. Efroni, L. Nathanson, Z. Barnes, et al., Altered immune pathway activity under exercise challenge in Gulf War Illness: an exploratory analysis, Brain Behav. Immun. 28 (2013) 159–169.
[88] J.P. O'Callaghan, L.T. Michalovicz, K.A. Kelly, Supporting a neuroimmune basis of gulf war illness, EBioMedicine 13 (2016) 5–6.
[89] L. Parkitny, S. Middleton, K. Baker, J. Younger, Evidence for abnormal cytokine expression in Gulf War Illness: a preliminary analysis of daily immune monitoring data, BMC Immunol. 16 (2015) 57.
[90] M. Di Filippo, D. Chiasserini, F. Gardoni, B. Viviani, A. Tozzi, C. Giampa, C. Costa, et al., Effects of central and peripheral inflammation on hippocampal synaptic plasticity, Neurobiol. Dis. 52 (2013) 229–236.
[91] S.N. Malaeb, J.M. Davis, I.M. Pinz, J.L. Newman, O. Dammann, M. Rios, Effect of sustained postnatal systemic inflammation on hippocampal volume and function in mice, Pediatr. Res. 76 (2014) 363–369.
[92] V. Chesnokova, R.N. Pechnick, K. Wawrowsky, Chronic peripheral inflammation, hippocampal neurogenesis, and behavior, Brain Behav. Immun. 58 (2016) 1–8.
[93] X. Zhu, M.H. Ji, S.M. Li, B. Li, L. Mei, J.J. Yang, Systemic inflammation impairs mood function by disrupting the resting-state functional network in a rat animal model induced by lipopolysaccharide challenge, Mediat. Inflamm. (2019) 6212934 2019.
[94] R. Dantzer, J.C. O'Connor, G.G. Freund, R.W. Johnson, K.W. Kelley, From inflammation to sickness and depression: when the immune system subjugates the brain, Nat. Rev. Neurosci. 9 (2008) 46–56.
[95] K. Ridder, S. Keller, M. Dams, A.K. Rupp, J. Schlaudraff, D. Del Turco, et al., Extracellular vesicle-mediated transfer of genetic information between the hematopoietic system and the brain in response to inflammation, PLoS Biol. 12 (2014) e1001874.
[96] J.J. Li, B. Wang, M.C. Kodali, C. Chen, E. Kim, B.J. Patters, et al., In vivo evidence for the contribution of peripheral circulating inflammatory exosomes to neuroinflammation, J. Neuroinflammation 15 (2018) 8.